520876
b.42

NASA/TM-2001-210828

Aerodynamic Measurements on a Large Splitter Plate for the NASA Langley Transonic Dynamics Tunnel

David M. Schuster
Langley Research Center, Hampton, Virginia

March 2001

The NASA STI Program Office ... in Profile

Since its founding, NASA has been dedicated to the advancement of aeronautics and space science. The NASA Scientific and Technical Information (STI) Program Office plays a key part in helping NASA maintain this important role.

The NASA STI Program Office is operated by Langley Research Center, the lead center for NASA's scientific and technical information. The NASA STI Program Office provides access to the NASA STI Database, the largest collection of aeronautical and space science STI in the world. The Program Office is also NASA's institutional mechanism for disseminating the results of its research and development activities. These results are published by NASA in the NASA STI Report Series, which includes the following report types:

- TECHNICAL PUBLICATION. Reports of completed research or a major significant phase of research that present the results of NASA programs and include extensive data or theoretical analysis. Includes compilations of significant scientific and technical data and information deemed to be of continuing reference value. NASA counterpart of peer-reviewed formal professional papers, but having less stringent limitations on manuscript length and extent of graphic presentations.

- TECHNICAL MEMORANDUM. Scientific and technical findings that are preliminary or of specialized interest, e.g., quick release reports, working papers, and bibliographies that contain minimal annotation. Does not contain extensive analysis.

- CONTRACTOR REPORT. Scientific and technical findings by NASA-sponsored contractors and grantees.

- CONFERENCE PUBLICATION. Collected papers from scientific and technical conferences, symposia, seminars, or other meetings sponsored or co-sponsored by NASA.

- SPECIAL PUBLICATION. Scientific, technical, or historical information from NASA programs, projects, and missions, often concerned with subjects having substantial public interest.

- TECHNICAL TRANSLATION. English-language translations of foreign scientific and technical material pertinent to NASA's mission.

Specialized services that complement the STI Program Office's diverse offerings include creating custom thesauri, building customized databases, organizing and publishing research results ... even providing videos.

For more information about the NASA STI Program Office, see the following:

- Access the NASA STI Program Home Page at ***http://www.sti.nasa.gov***

- E-mail your question via the Internet to help@sti.nasa.gov

- Fax your question to the NASA STI Help Desk at (301) 621-0134

- Phone the NASA STI Help Desk at (301) 621-0390

- Write to:
  NASA STI Help Desk
  NASA Center for AeroSpace Information
  7121 Standard Drive
  Hanover, MD 21076-1320

NASA/TM-2001-210828

Aerodynamic Measurements on a Large Splitter Plate for the NASA Langley Transonic Dynamics Tunnel

David M. Schuster
Langley Research Center, Hampton, Virginia

National Aeronautics and
Space Administration

Langley Research Center
Hampton, Virginia 23681-2199

March 2001

Available from:

NASA Center for AeroSpace Information (CASI)
7121 Standard Drive
Hanover, MD 21076-1320
(301) 621-0390

National Technical Information Service (NTIS)
5285 Port Royal Road
Springfield, VA 22161-2171
(703) 605-6000

ABSTRACT

Tests conducted in the NASA Langley Research Center Transonic Dynamics Tunnel (TDT) assess the aerodynamic characteristics of a splitter plate used to test some semispan models in this facility. Aerodynamic data are analyzed to determine the effect of the splitter plate on the operating characteristics of the TDT, as well as to define the range of conditions over which the plate can be reasonably used to obtain aerodynamic data. Static pressures measurements on the splitter plate surface and the equipment fairing between the wind tunnel wall and the splitter plate are evaluated to determine the flow quality around the apparatus over a range of operating conditions. Boundary layer rake data acquired near the plate surface define the viscous characteristics of the flow over the plate. Data were acquired over a range of subsonic, transonic and supersonic conditions at dynamic pressures typical for models tested on this apparatus. Data from this investigation should be used as a guide for the design of TDT models and tests using the splitter plate, as well as to guide future splitter plate design for this facility.

SYMBOLS

C	Equipment fairing chord, inches
C_p	Pressure coefficient $\left(\frac{p - p_\infty}{q_\infty}\right)$
M	Mach number
p	Pressure, psf
p_∞	Freestream static pressure, psf
q	Dynamic pressure, psf
q_∞	Freestream dynamic pressure, psf
V	Velocity, ft./sec.
V_∞	Freestream velocity, ft./sec.
X	Streamwise distance along plate, inches
Y	Distance perpendicular to plate surface, inches
α	Angle-of-attack, degrees
δ	Boundary layer thickness, inches

INTRODUCTION

The NASA Langley Transonic Dynamics Tunnel (TDT) recently completed a substantial Construction of Facility (CofF) project that converted the heavy gas operating medium for the tunnel from R-12 to the more environmentally safe R-134a. The TDT is a large-scale, closed-return, continuous flow tunnel capable of operating at subsonic through low supersonic speeds. An aerial view of the tunnel is presented in Figure 1. Reference 1 presents a detailed description of the heavy gas conversion project and an overview of the TDT in general. At the completion of this CofF project, a substantial wind tunnel calibration effort was undertaken. One phase of this effort was to investigate the flow characteristics about a splitter plate mounting system previously used in the TDT. This report documents the testing and analysis of the splitter plate data taken during this calibration phase.

The subject splitter plate is designed to provide a semispan model mounting surface that shields dynamic model mounting hardware, such as a pitch and plunge apparatus (PAPA), from the tunnel flow and simulates a plane of flow symmetry. A number of semispan models have been tested on this apparatus, most notably the NASA LaRC Benchmark Models Program wings[2-5] and the DARPA/AFRL/NASA Smart Wing[6]. The overall concept behind the splitter plate is to reduce the thickness of the boundary layer along the surface against which the model is mounted by effectively starting a new boundary layer just ahead of the model. This is accomplished by placing the splitter plate in the freestream flow of the test section outside the wind tunnel wall boundary layer, as shown in Figure 2. In this figure, it can be seen that the boundary layer thickness, δ, that would be encountered by the model on the splitter plate is much smaller than if the model were mounted directly to the wind tunnel wall, since the boundary layer has a much shorter distance over which to grow. Thus a significantly larger percentage of the model is in freestream flow when it is mounted on the splitter plate.

To date, no attempt to evaluate the flow about this splitter plate has been accomplished and little is known about the nature of the pressure distribution or the development of the boundary layer along the plate. To produce a representative plane of symmetry, the splitter plate boundary layer in the vicinity of the model must be thin and no significant pressure gradients should be present in the model mounting vicinity. In addition, data from previous semispan tests involving the splitter plate indicate that the plate and its mounting hardware add a significant blockage to the flow in the tunnel. This is evidenced by the fact that the upper Mach number limit of the TDT is significantly decreased when the splitter plate is installed. This blockage can also increase the flow angularity in the test section. These issues will be addressed, and their importance evaluated, through the analysis of the experimental data acquired during this test.

There are four primary objectives of this investigation:

1) Quantify the flow characteristics on the splitter plate surface as a function of the flow conditions.

2) Specify ranges of operation in which tests involving models mounted on the plate can reasonably expect to obtain accurate quantitative data.

3) Assess the impact of the splitter plate on the operating characteristics of the TDT.

4) Recommend modifications to the existing plate hardware and/or new splitter plate configurations that might further improve the TDT flow quality and extend the operating range of the tunnel for this type of testing.

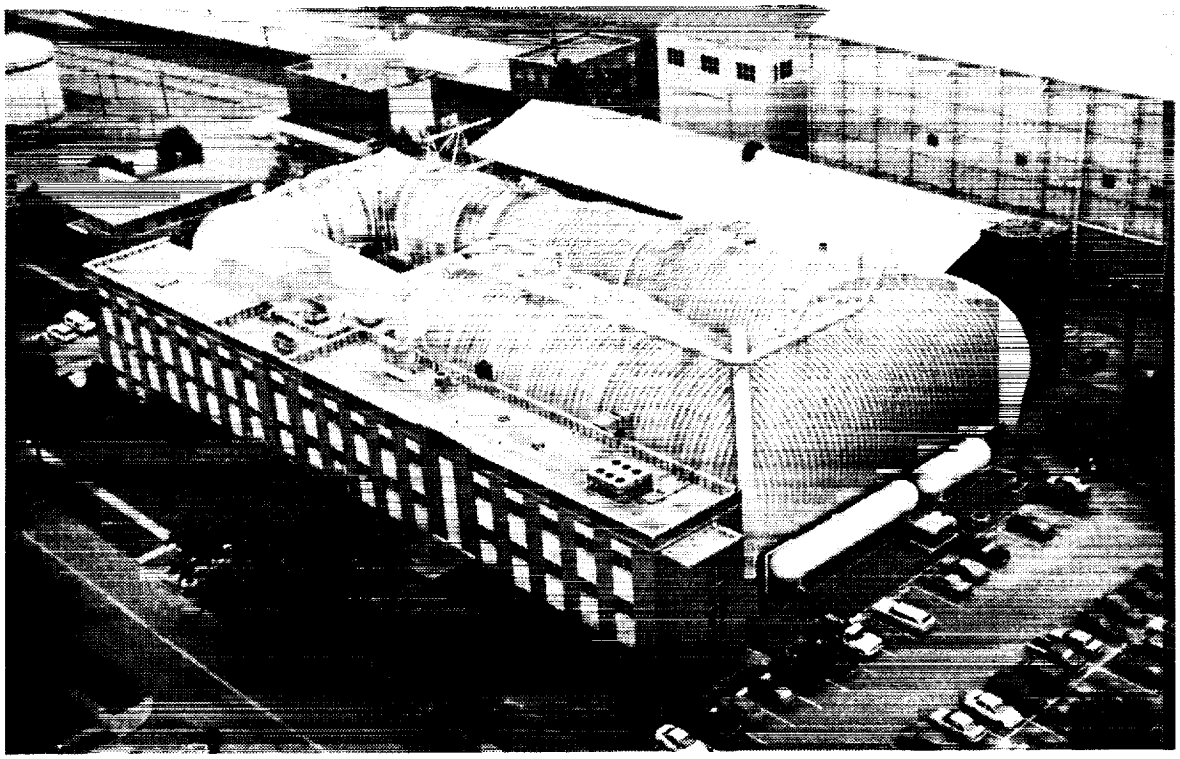

Figure 1. NASA Langley Research Center Transonic Dynamics Tunnel.

Top View of TDT East Wall and Splitter Plate

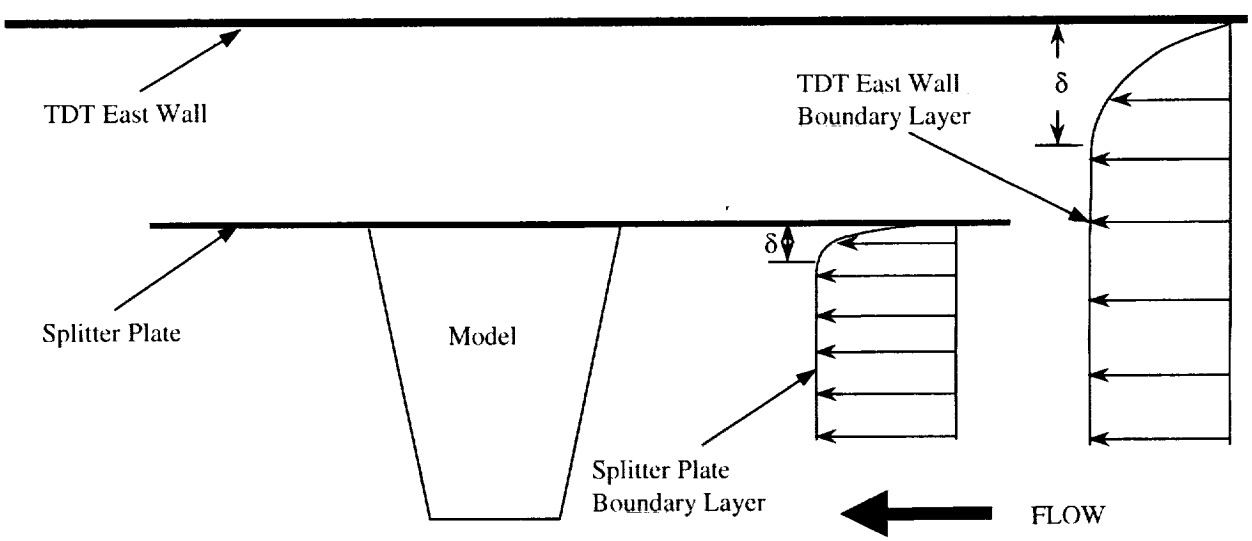

Figure 2. Adding a splitter plate reduces boundary layer thickness experienced by the model.

To address these objectives, an experimental program was developed to test the splitter plate in the TDT without an accompanying aerodynamic model. This investigation was conducted over a two-week period in June 1998 as TDT Test 527. Data from this test clearly defines areas where the plate is and is not suitable for aerodynamic testing. Analyses of the data also suggest methods that might improve the performance of the TDT with the plate installed, and extend the operational range over which the plate can be used to acquire accurate aerodynamic data.

The remainder of this report is broken into four main sections beginning with a discussion of the test procedure. This section includes a description of the test setup and configuration, instrumentation, flow conditions of interest, and test matrix. Test results are presented and discussed in the next section. The impact of the splitter plate on the TDT operating envelope is evaluated. A detailed discussion of the surface pressure distribution along the plate is presented and comparisons with computed data are analyzed. The boundary layer near the typical model mounting position is characterized, and pressure distributions obtained on the equipment fairing are evaluated. A set of guidelines and recommendations for future testing using this splitter plate are presented in the next section, and concluding remarks are presented in the final section.

TEST PROCEDURE

A test plan was developed that involved the measurement of static pressures and boundary layer profiles on the surface of the splitter plate, as well as static pressure measurements on the equipment fairing behind the plate. An experiment was performed for a range of flight conditions typical for splitter plate testing. Tests were performed in both air and R-134a.

Test Configuration

The splitter plate, without an accompanying aerodynamic model, was mounted in the TDT test section using standard procedures for this device. The complete apparatus, shown in Figure 3, is composed of a series of one-half inch thick aluminum sections that are bolted together to form the complete 144 in. wide by 120 in. tall plate. Models are typically mounted with their center 84 in. from the leading edge of the plate. The plate is mounted to the sidewall of the TDT by a set of 24 beams that place the mounting surface of the plate approximately 40 in. from the TDT east wall. Recent measurements of the sidewall boundary layer show it to be approximately 12 in. thick for the empty tunnel configuration, which places the splitter plate well into the tunnel freestream flow. The splitter plate support beams are arranged in a 5 x 5 matrix with the center beam in the matrix replaced by the equipment fairing. This component functions primarily as an aerodynamic fairing that shields instrumentation and mounting hardware running between the splitter plate and the TDT sidewall from tunnel flow passing behind the splitter plate. The equipment fairing is composed of sheet metal sections that are assembled into a symmetrical airfoil shape loosely patterned after a 37.5% thick biconvex airfoil section. All of the TDT wall slots were open during testing. This is the standard tunnel configuration used for testing with the splitter plate installed.

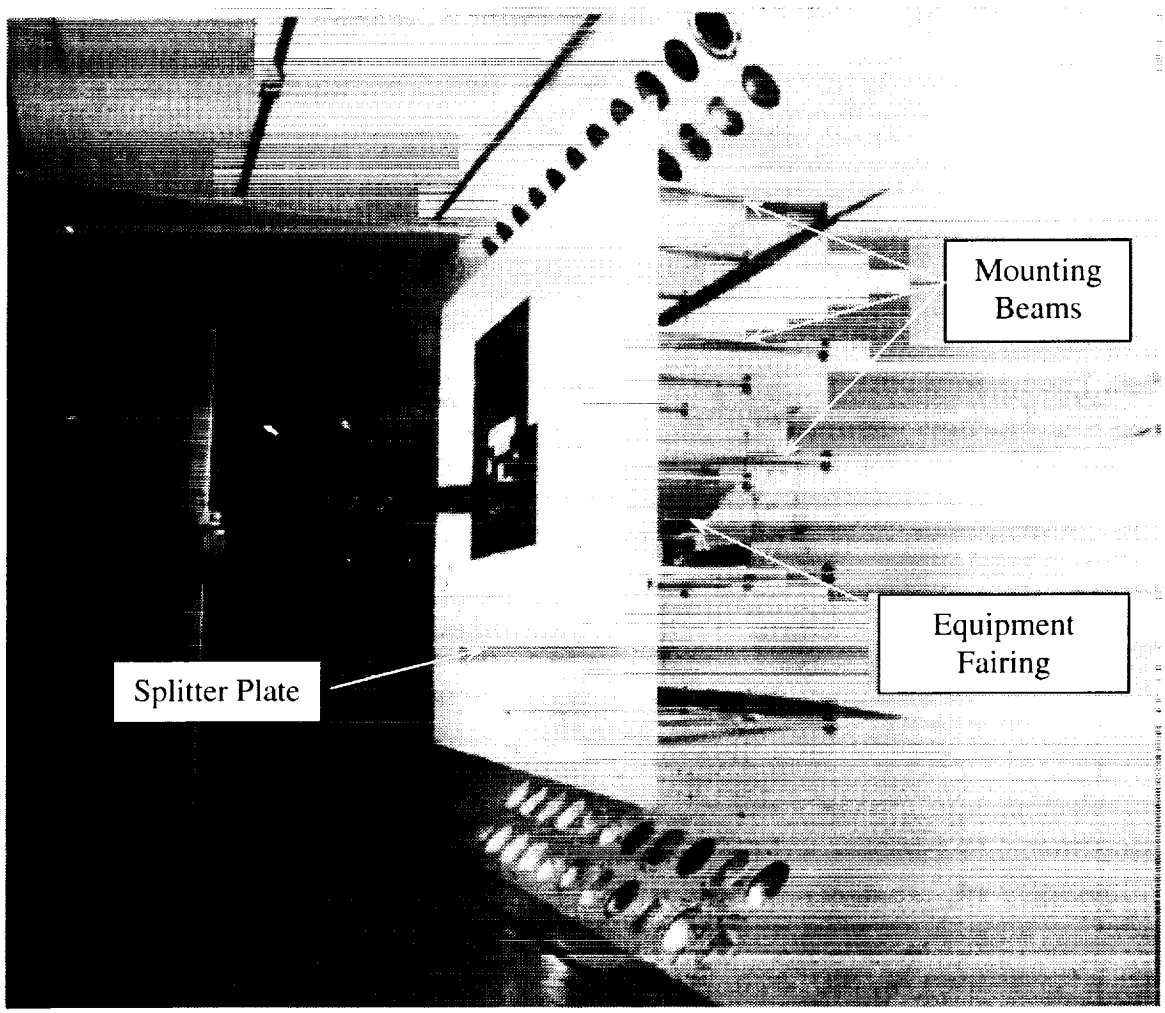

Figure 3. Splitter plate installed in TDT with a test wing.

Instrumentation

The splitter plate was instrumented with static pressure ports on the plate surface and on the centerline of the equipment fairing, and a rake of total pressure ports that measured the boundary layer in the vicinity of the model mounting location. Figure 4 shows a schematic of the splitter plate and the instrumentation on its surface. Three streamwise rows of static pressure ports were installed on the plate. The top and bottom rows each contain 13 ports, while the center row contains a denser distribution of 17 ports. The orifice locations, measured from the leading edge of the plate, are tabulated in the figure. The boundary layer rake was located midway between the lower and middle row of pressure ports at the streamwise location of the model center on the plate.

The boundary layer rake is shown in Figure 5. The rake is constructed of stainless steel, has a tapered planform, and a faceted airfoil section. Both the rake planform and the airfoil cross-section at the lower edge of the rake are shown in the figure. Attached to the leading edge of the rake are 28 total pressure tubes, distributed as shown. The first five tubes are 0.040 in. ID, 0.060 in. OD stainless steel, while the rest of the tubes are 0.060 in. ID, 0.090 in. OD stainless steel.

A top view of the experimental setup is shown in Figure 6. This view shows the approximate locations of the static pressure ports on the equipment fairing. The actual streamwise location of the upper and lower surface ports is tabulated in the figure. The distribution of ports was selected in an attempt to capture expected shock waves and areas of separated flow on the fairing surface. The distribution of ports on the upper and lower surface is not identical due to constraints presented by the construction of the equipment fairing.

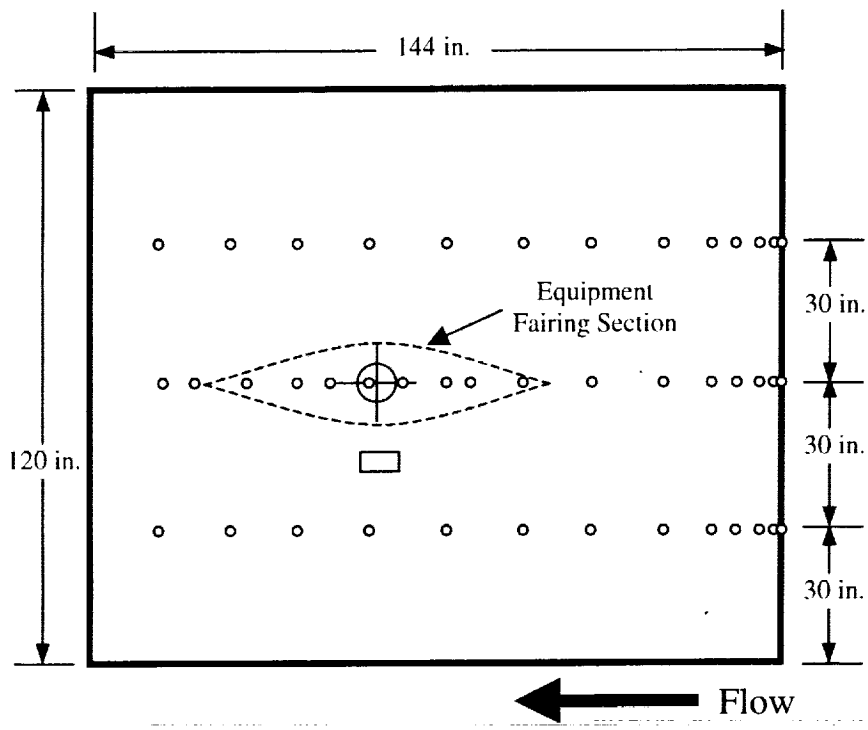

Pressure Orifice Locations (Measured from the leading edge of plate, in.)	
Middle Row	Top/Bottom Row
0.38	0.38
2.00	2.00
5.00	5.00
9.75	10.00
15.00	15.00
25.00	25.00
39.75	40.00
54.00	54.00
65.00	
70.00	70.00
79.00	
86.00	86.00
94.00	
101.00	101.00
111.50	115.00
122.20	
129.00	130.00

Figure 4. Pressure instrumentation layout for the splitter plate surface.

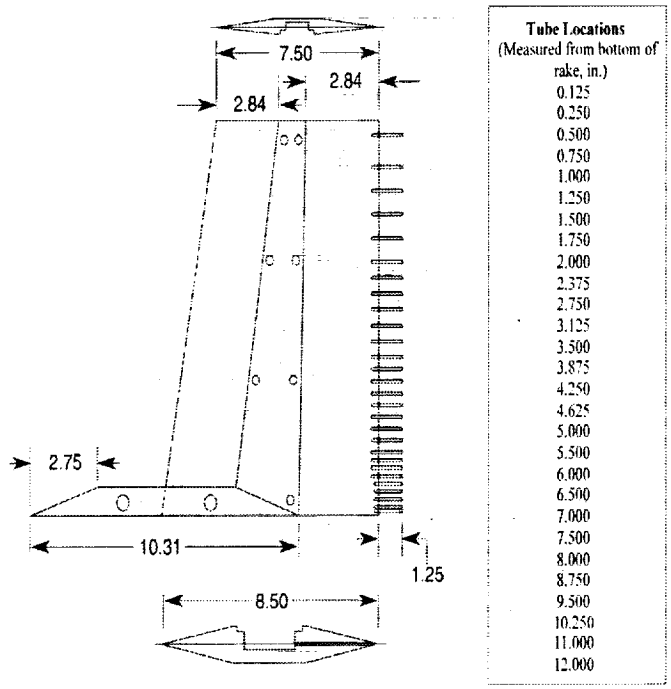

Figure 5. Boundary layer rake instrumentation schematic.

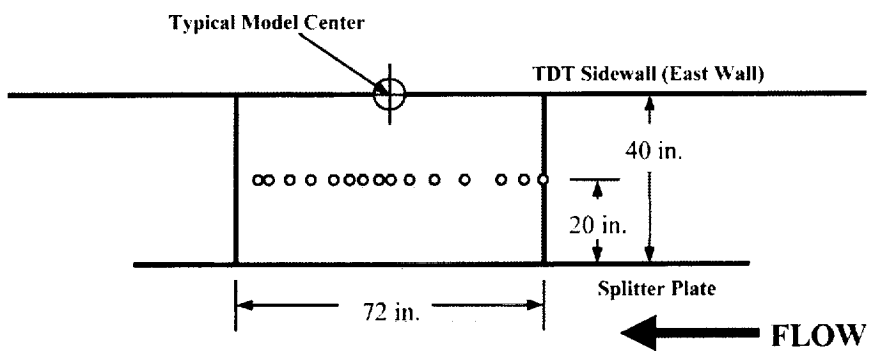

Fairing Orifice Locations (Measured from Fairing L.E.)			
Upper Surface		Lower Surface	
X(in.)	X/C	X(in.)	X/C
2.39	0.033	2.39	0.033
6.74	0.094	6.74	0.094
12.06	0.168	12.15	0.169
20.69	0.287	20.87	0.290
27.75	0.385	26.01	0.361
33.48	0.465	33.57	0.466
37.84	0.526	37.93	0.527
40.59	0.564	40.68	0.565
44.35	0.616	44.54	0.619
47.47	0.659	47.65	0.662
51.23	0.712	50.32	0.699
56.55	0.785	56.00	0.778
61.51	0.854	60.82	0.845
66.41	0.922	65.63	0.912
68.69	0.957	68.11	0.946

Figure 6. Top view of splitter plate and instrumentation equipment fairing.

Each of the pressure ports on the splitter plate, boundary layer rake, and equipment fairing were sampled using the Pressure Systems Electronically Scanned Pressure (ESP) System 8400. A total of seven 16-channel ESP modules were required for this test. Three +/- 1.5 psi modules were used to sample the pressures on the plate, two +/- 2.5 psi modules were attached to the equipment fairing ports, and two +/- 5.0 psi modules were attached to the boundary layer rake. The pressure range of the modules was selected based on the anticipated differential pressure to be encountered on each of the test components.

The reference pressures for each module were combined to measure a single reference pressure that was measured in the tunnel plenum chamber. The plenum chamber pressure is also used as the tunnel static pressure when computing flow condition parameters. In this configuration, the ESP system measures the differential pressure between the port and the freestream static pressure. The pressure coefficient, C_p, is computed by normalizing the measured differential pressure at each port by the freestream dynamic pressure. The local Mach number was also calculated from the static pressure data using the program that calculates the tunnel parameters for the TDT. The effect of the test gas purity is included in the computation of the local Mach number. The static pressure coefficient and the local Mach number are the primary reduced quantities that are extracted from the splitter plate and equipment fairing static pressure data for further analysis. The boundary layer rake data is reduced similarly. However in this case, the freestream static pressure, stagnation temperature, and test gas purity are used in conjunction with the measured total pressure data from the rake to compute the ratio of the local velocity to the freestream velocity.

Since the boundary layer rake could potentially influence the static pressure measurements on the splitter plate surface, two configurations, clean plate and plate with rake, were tested at each tunnel condition. These were the only configurations tested during this investigation.

Flow Conditions and Test Matrix

Test conditions for this investigation were selected by reviewing conditions for previous tests involving the splitter plate, and anticipated future test requirements for this device. The maximum dynamic pressure at which the splitter plate had been previously cleared for operation in the TDT is 200 psf, so this was established as an upper limit for this test. In addition, the majority of past tests had been conducted in heavy gas at dynamic pressures in the range of 150 – 180 psf. Given this information, testing in R-134a at a dynamic pressure of 170 psf was established as the first priority for this test. Air testing at a dynamic pressure of 150 psf was established as a second priority.

The TDT operating envelope in R-134a is shown in Figure 7. The area designated by the heavy lines is the range over which the majority of data were taken during this test. The operating envelope for air is shown in Figure 8 with the test conditions similarly designated. Tests performed in R-134a are presented in matrix format in Tables 1, 2, and 3. Tables 1 and 2 cover the test conditions described in Figure 7 for the clean plate and plate with boundary layer rake configurations, respectively. Table 3 shows the points taken during the definition of the TDT upper Mach number limit with the clean plate configuration. Tables 4 and 5 list the data taken in air for the clean splitter plate and the splitter plate with boundary layer rake configuration. No investigation of the upper Mach number limit in air was conducted.

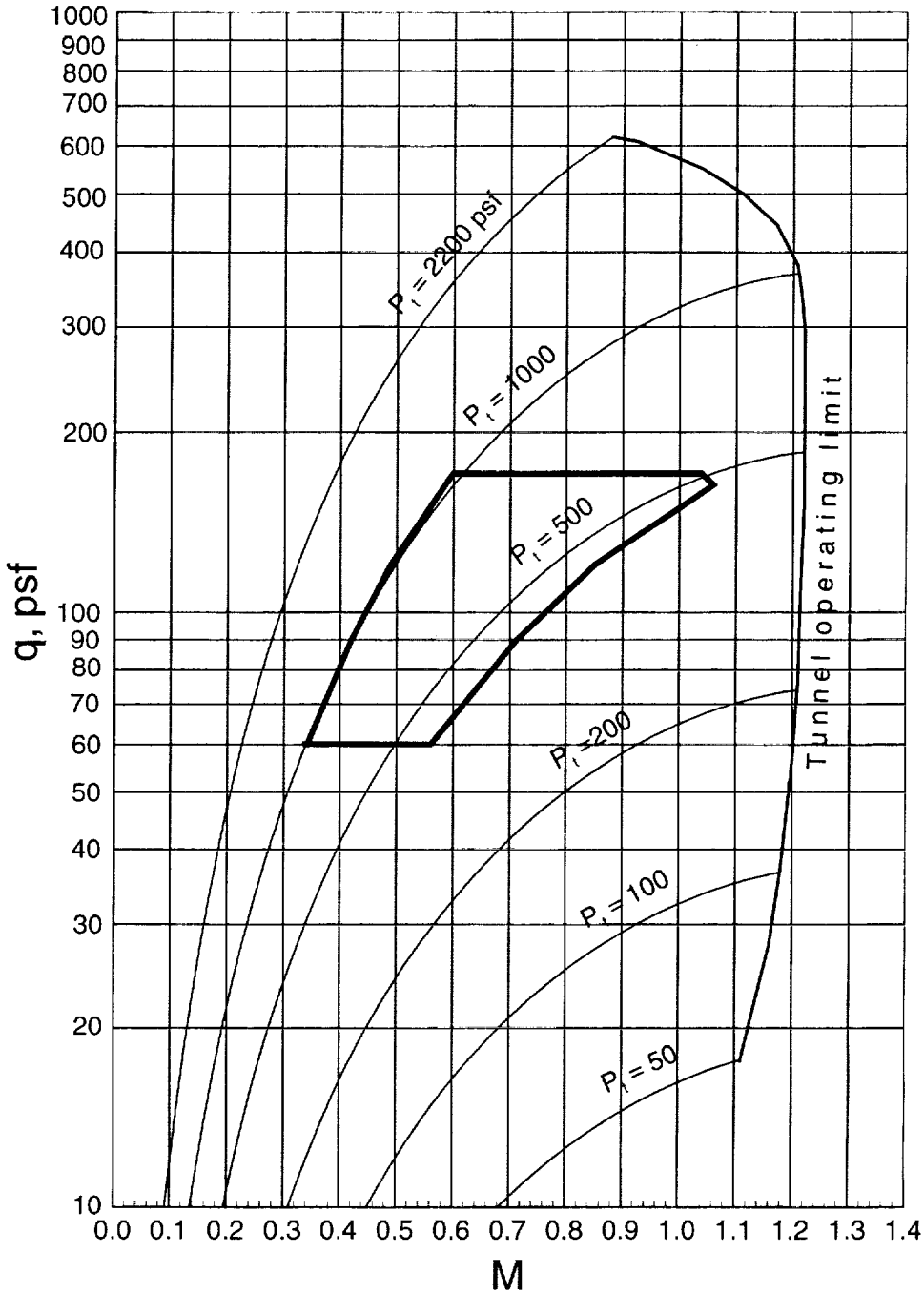

Figure 7. Test program shown in TDT operating envelope for R-134a test medium.

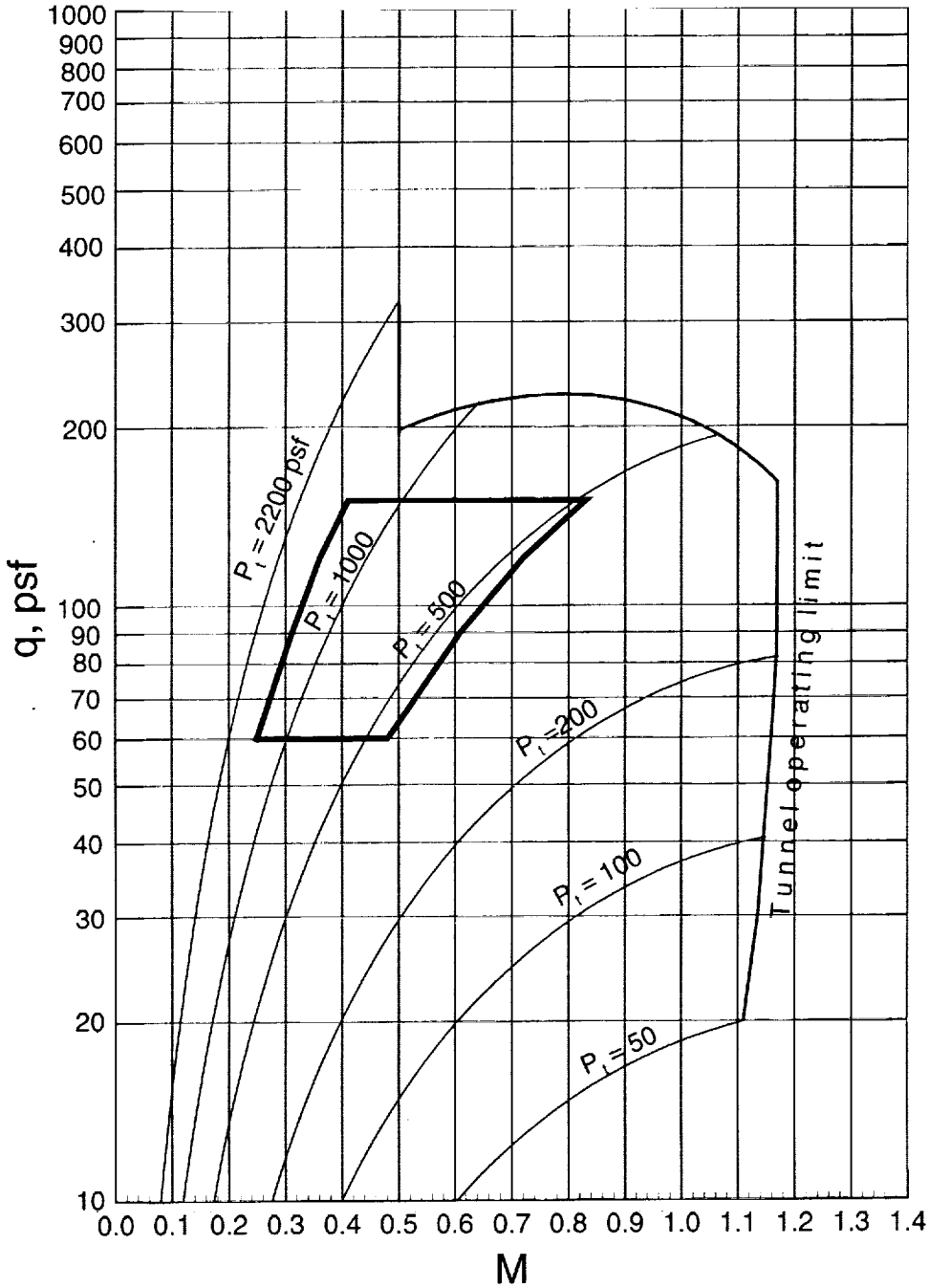

Figure 8. Test program shown in TDT operating envelope for air test medium.

Table 1. Test matrix for clean splitter plate in R-134a test medium.

Mach	q (psf)	Run	Tab
0.60	170	6	181
0.70	170	6	175
0.80	170	6	170
0.85	170	6	168
0.90	170	6	167
0.96	170	6	166
0.98	170	6	164
1.01	165	6	163
1.04	170	6	162
1.06	163	6	160
0.49	120	6	182
0.57	120	6	176
0.65	120	6	171
0.85	120	6	157
0.42	90	6	183
0.49	90	6	177
0.55	90	6	172
0.71	90	6	156
0.34	60	6	185
0.39	60	6	179
0.44	60	6	173
0.56	60	6	155

Table 2. Test matrix for splitter plate with boundary layer rake in R-134a test medium.

Mach	q (psf)	Run	Tab
0.60	170	8	244
0.70	170	8	239
0.80	170	8	234
0.85	170	8	231
0.90	170	8	230
0.95	170	8	228
0.98	170	8	227
1.01	170	8	226
1.05	168	8	225
0.49	120	8	245
0.57	120	8	240
0.65	120	8	235
1.05	120	8	222
0.42	90	8	246
0.49	90	8	241
0.55	90	8	236
1.04	90	8	221
0.34	60	8	247
0.39	60	8	242
0.44	60	8	237
0.87	60	8	217

Table 3. Test matrix for TDT tunnel boundary definition with splitter plate in R-134a test medium.

Mach	q (psf)	Run	Tab
1.04	77	8	219
1.04	90	8	221
1.05	121	8	222
1.05	149	8	224
1.05	168	8	225

Table 4. Test matrix for clean splitter plate in air test medium.

Mach	q (psf)	Run	Tab
0.41	150	4	121
0.50	150	4	115
0.60	150	4	110
0.70	150	4	108
0.80	150	4	107
0.83	150	4	106
0.36	120	4	120
0.53	120	4	111
0.72	120	4	105
0.31	90	4	119
0.45	90	4	112
0.61	90	4	104
0.25	60	4	118
0.36	60	4	114
0.48	60	4	103

Table 5. Test matrix for splitter plate with boundary layer rake in air test medium.

Mach	q (psf)	Run	Tab
0.50	150	3	79
0.60	150	3	74
0.70	150	3	69
0.80	150	3	67
0.84	150	3	64
0.35	120	3	83
0.53	120	3	75
0.61	120	3	70
0.70	120	3	68
0.72	120	3	63
0.30	90	3	84
0.45	90	3	76
0.52	90	3	71
0.61	90	3	62
0.25	60	3	85
0.36	60	3	77
0.42	60	3	72
0.48	60	3	61

RESULTS AND DISCUSSION

The aerodynamic data acquired during this test has been analyzed and categorized into four major areas of interest. The most obvious impact of the splitter plate on the aerodynamics of the TDT is the decrease in the upper Mach number limit of the tunnel when the plate is installed. A number of test points were taken and analyzed to quantify this effect. The second set of analyses focuses on the pressure distributions along the splitter plate. These data are evaluated to define the flow conditions over which reasonable aerodynamic model data can be acquired and to investigate potential problems with local flow angularity due to blockage. The data from the boundary layer rake is analyzed to estimate the boundary layer thickness at the model location as a function of flow condition. Finally, the pressure distribution on the equipment fairing is investigated to determine some of the characteristics of the flow behind the splitter plate, and its potential impact on the overall flow in the test section. Each of these issues is discussed in detail in the following sections.

TDT Operating Envelope Limits with Splitter Plate

The splitter plate is mounted approximately 40 inches from the TDT east wall by a matrix of 24 rods, and the equipment fairing. The plate and mounting hardware for this apparatus contribute a significant amount of blockage to the flow in the TDT test section. This blockage can have a number of adverse effects on the flow that can limit the conditions at which aerodynamic models can be effectively tested. The quantification of these limitations is one purpose of this research. The most easily measured blockage effect is the decrease in the upper Mach number limit for the TDT with the plate installed. Cursory quantification of this limit has been attempted in other tests involving the splitter plate, but these evaluations always included an aerodynamic model. Therefore, this effort quantifies the tunnel blockage effects due solely to the plate. Since the majority of transonic testing with the splitter plate occurs in the R-134a test medium, the upper Mach number limit was investigated only for R-134a.

The TDT Mach number limit was determined by increasing the tunnel drive to its maximum speed. Vanes ahead of the tunnel fan, known as prerotation vanes, can then be adjusted to further increase the Mach number in the test section. As shown in Table 3, this procedure results in a Mach number of 1.04 at a dynamic pressure of 77 psf. A series of points were then taken where additional R-134a is bled into the tunnel circuit to increase the density and dynamic pressure of the flow. During this series of points, the Mach number increased slightly to 1.05 at 177 psf. In Figure 9, the measured limit with the splitter plate installed is compared with the empty tunnel limit for the TDT. In the empty tunnel, the upper Mach limit is approximately 1.2 at dynamic pressures between 70 and 170 psf. The 12.5% reduction in the maximum Mach number from Mach 1.2 to 1.05 is due to the physical and aerodynamic blockage of the splitter plate and its mounting system.

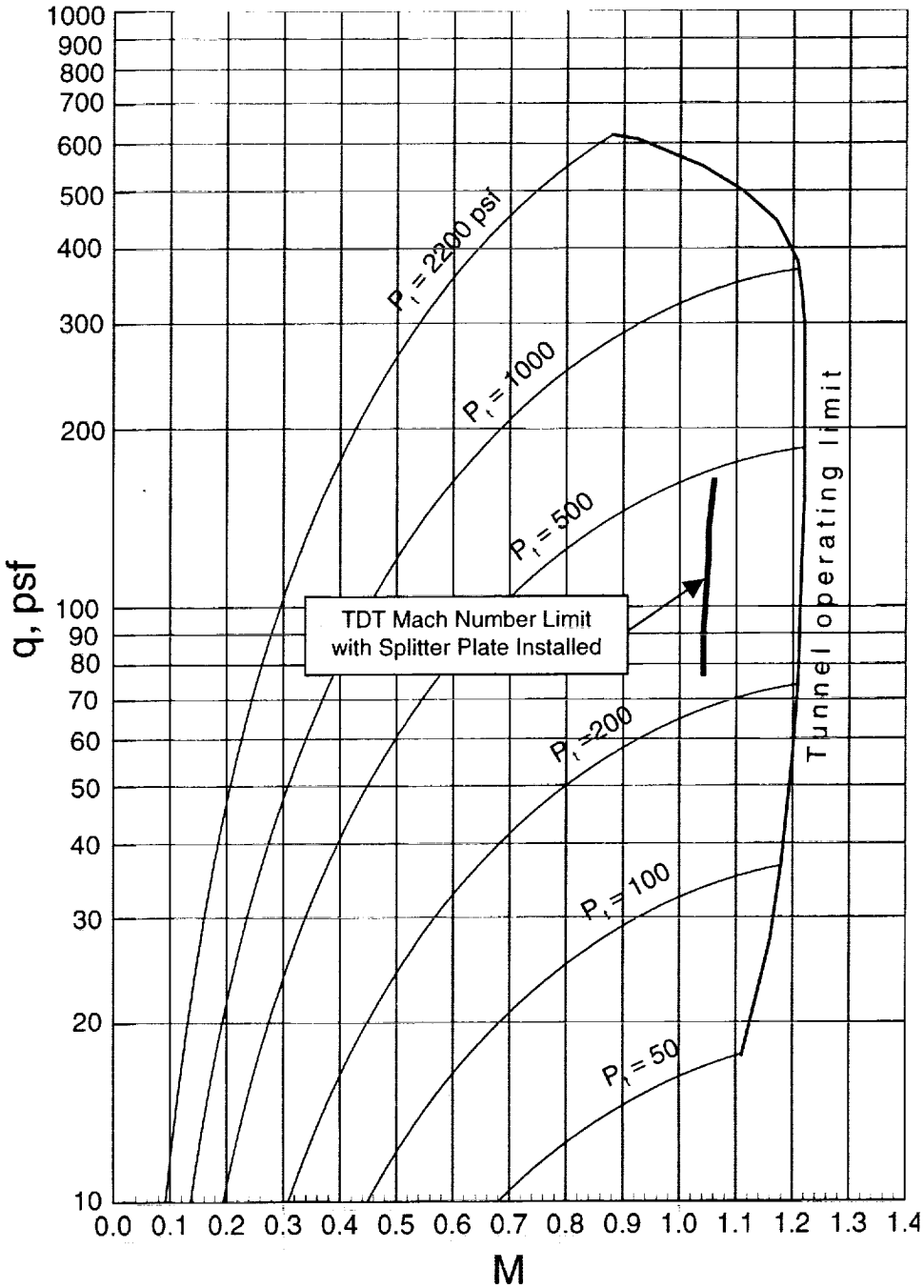

Figure 9. TDT R-134a operating envelope with splitter plate Mach number limitation.

The frontal area of the plate and its mount account for the physical blockage and while this blockage is not negligible at approximately 4% of the test section cross-sectional area, the large reduction in Mach number capability suggests that aerodynamic blockage plays a significant role in this reduction. Aerodynamic blockage arises from shock waves, boundary layers, and/or separated flow generated by the mounting system. These phenomena can reduce the area through which the test gas can flow. Typical test configurations for the TDT, with the splitter plate installed, include having all of the slots in the wind tunnel walls open. This provides an alternate path for flow through the plenum chamber and helps mitigate blockage problems. However, in this case, it appears that an improved aerodynamic design of the plate and its mounting system may have significant potential for improving the maximum Mach number capability of the tunnel with the splitter plate installed.

Splitter Plate Surface Pressure Distribution

An important aspect of the flow in the vicinity of any semispan model is the nature of the pressure distribution on the wall that the model is mounted upon. It is critical that there be no pressure gradients along the wall, or in this case the clean splitter plate. It is also important that the pressure along the wall be as close to the freestream static pressure as possible. Given these criteria, the pressure distributions on the splitter plate surface can tell us under which flow conditions it is appropriate to use the splitter plate for wind tunnel model testing.

The clean splitter plate, i.e. without the boundary layer rake installed, was tested in both R-134a and air. The air data exhibits similar behavior to the R-134a data, so only the latter will be discussed in the remainder of this report. The majority of data were taken at a freestream dynamic pressure of 170 psf, with more limited investigations at 60, 90, and 120 psf. Again, the pressure distributions at the lower dynamic pressures exhibit similar trends to those at 170 psf, and they are excluded from this discussion. At the 170 psf dynamic pressure, Mach numbers were evaluated ranging from 0.6 to 1.05.

At subcritical Mach numbers, the splitter plate performs as expected. Figure 10 shows the surface pressure distribution along the splitter plate measured from the plate leading edge at Mach 0.6 and a dynamic pressure of 170 psf. Models are typically centered on the splitter plate 84 inches from the leading edge and this point is designated with the arrow in the figure. It is in this area that the pressure should be near freestream ($C_p = 0.0$), and the pressure gradients should be small. At this Mach number, this is effectively the case. The middle row point at 94 inches and the lower row point at 70 inches are the only points in the vicinity of the model center that deviate significantly from the freestream pressure. This section of the plate is designed to be removable and tailored to the specific model to be tested. The removable section used in this test was adapted from a previous test and is constructed of honeycomb. There were several imperfections in the surface of the plate that were noted during testing. Specifically, the honeycomb was dimpled in the vicinity of the 94-inch pressure port, which probably accounts for the deviation in pressure at this point. Attention to the surface of the plate near the model would likely eliminate these local anomalies in the pressure.

Flow angularity in the tunnel generated by the installation of the splitter plate was also an objective of this investigation. Close examination of Figure 10 shows a noticeable suction peak, characterized by the negative pressure coefficient, near the splitter plate leading edge. It was initially speculated that this pressure peak was caused by local flow angularity resulting from the blockage of the plate. Subsequent inviscid analyses of the plate using the CAP-TSD transonic small disturbance code showed that this was not the case, and that the local leading edge geometry of the plate was responsible for generating this significant pressure peak. Figure 11 compares two CAP-TSD analyses on a zero-thickness two-dimensional flat plate with TDT data along the middle pressure row of taps at 0.6 Mach number. The

first CAP-TSD solution is at zero degrees angle-of-attack, and as expected for a theoretical analysis, predicts a plate pressure distribution which is identically aligned with the x-axis at $C_p = 0.0$. The second analysis is at an angle-of-attack of 0.5 degrees and generates a suction peak at the leading edge of the plate due to the local acceleration of the flow around the sharp leading edge. However, this analysis also predicts that there will be a pressure gradient along a significant portion of the plate. Even at just 0.5 degrees angle-of-attack, the analysis predicts that there will be a noticeable pressure gradient at the model location. Overall, the correlation between theory and experiment for this case is not good and suggests that this simple flat plate model of the splitter plate may not be sufficient for correlation with TDT data.

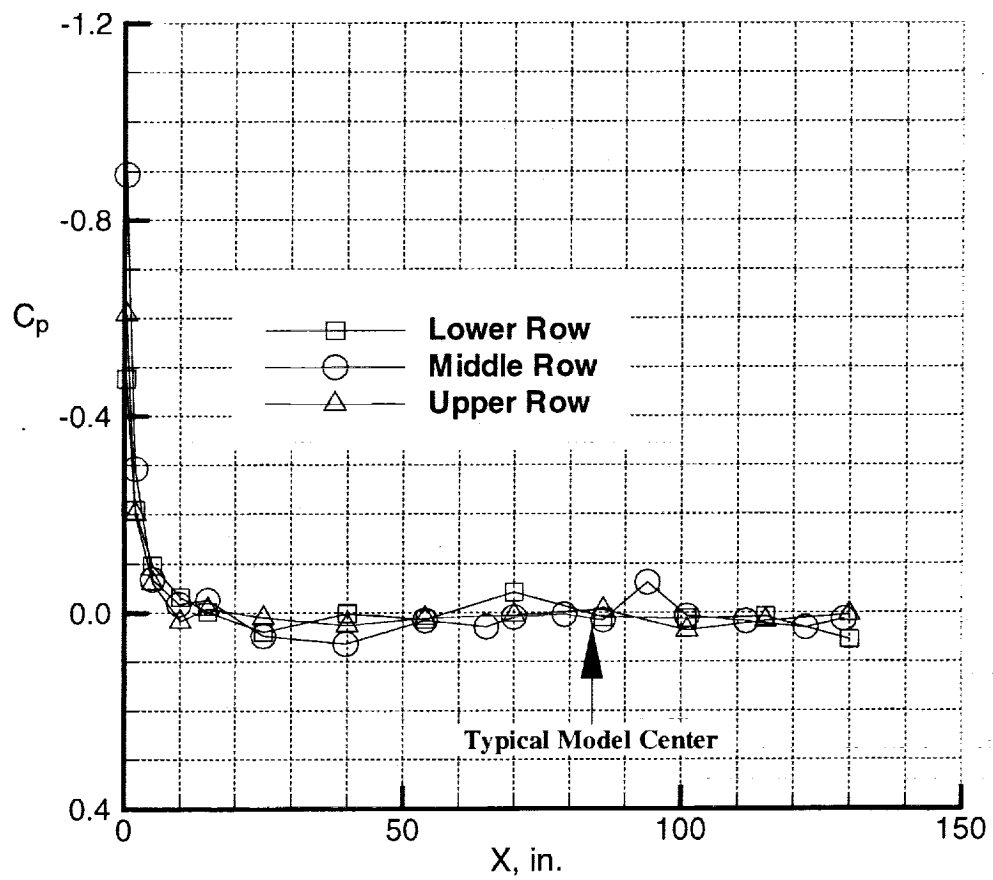

Figure 10. TDT splitter plate surface pressure distribution at M=0.60, q=170psf in R-134a.

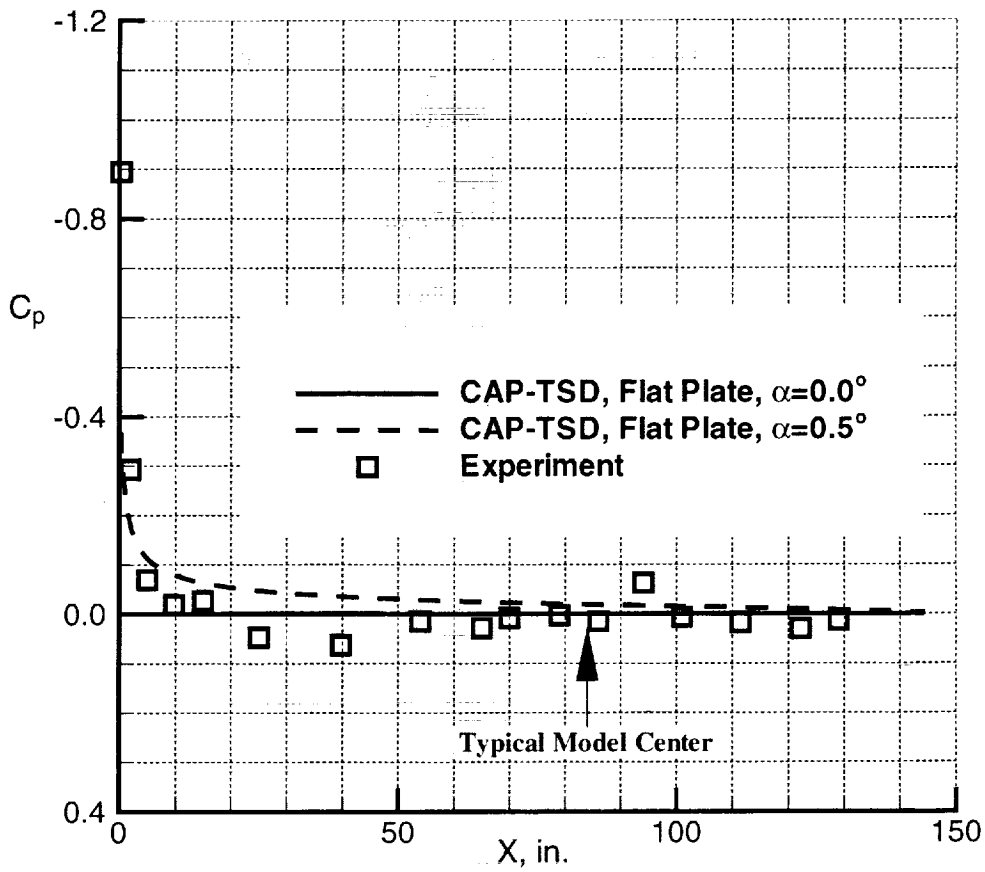

Figure 11. Comparison of CAP-TSD flat plate analysis with TDT data at M = 0.60, q=170 psf in R-134a.

The splitter plate leading edge geometry consists of a 30° included angle wedge with a 0.06 in. leading edge radius as shown in Figure 12. This geometry can be accurately modeled in CAP-TSD, and a refined model of the splitter plate, including the wedge leading edge was developed for the theoretical analysis. Figure 13 shows the resulting CAP-TSD analysis at Mach 0.6 for this updated model. In this case, the theoretical angle-of-attack is zero degrees, and the analytical data compares much more favorably with that obtained in the TDT. The pressure distribution in the leading edge region is accurately predicted by CAP-TSD, and this trend is repeated throughout the Mach number range. **Therefore, for the primary conditions of interest, the leading edge shape of the plate plays a significant role in the pressure distribution on the forward part of the splitter plate, and flow angularity at the plate leading edge is negligible.**

The experimental data at the 25 and 30 in. locations consistently show a pressure larger than the freestream pressure. This trend is seen at all Mach numbers, and could be due to an imperfection in the plate, external loads on the plate causing it to deform in this region, or some type of aerodynamic interference. A local deformation of the plate, possibly due to its mounting on the east wall of the TDT, seems the most likely reason for this rise in pressure. Regardless of the source of the deviation, it is observed at all conditions, and at the higher Mach numbers becomes problematic to the downstream flow on the plate.

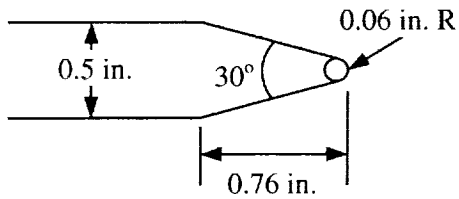

Figure 12. Splitter plate leading edge geometry detail.

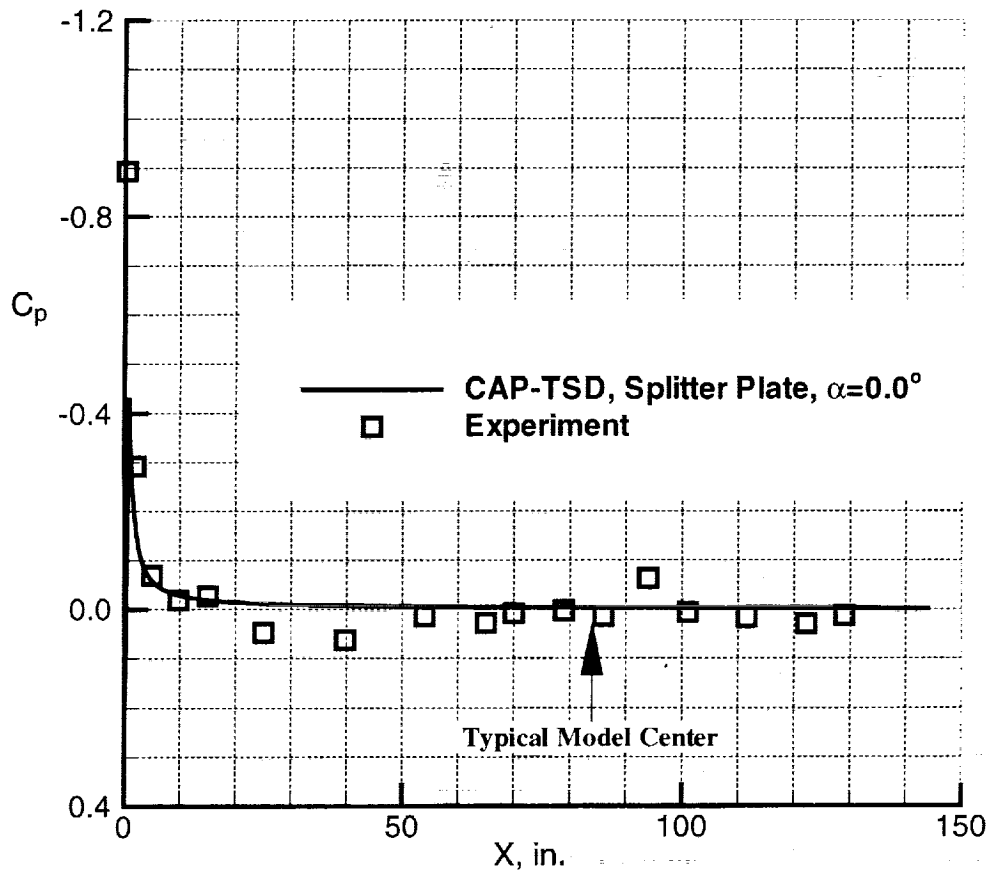

Figure 13. Comparison of CAP-TSD and TDT data for accurate splitter plate geometry model at M=0.60, q=170 psf in R-134a.

The pressure distribution along the center of the plate at Mach 0.8 is shown in Figure 14. Again, both CAP-TSD inviscid computations and experimental data are presented at this flow condition. The characteristics of the pressure distribution for this case are similar to those at Mach 0.6, and CAP-TSD reasonably predicts the pressures on the splitter plate, especially near the leading edge and at the model location. The increase in pressure in the 20-50 in. region along the plate is also more prominent at this Mach number. However, the most important feature to note about this condition is that the local Mach number derived from the experimental pressure in the vicinity of the plate leading edge reaches a supersonic value on the order of 1.1. At Mach 0.7 the Mach number distribution remained entirely subsonic, so the Mach 0.8 condition is the first point where locally supercritical Mach numbers were observed along the plate. Local supercritical flow that is decelerated to subsonic conditions at the model location provides potential for total pressure losses downstream of the supersonic region, primarily due to the presence of shock waves. At the Mach 0.8 condition, the flow is only slightly supersonic at the leading edge, and shock waves will be weak, if they exist at all. Therefore the total pressure losses will likely be insignificant at these conditions. At higher Mach numbers however, the shocks are much stronger, and the total pressure losses can no longer be ignored. **Thus it is recommended that aerodynamically meaningful testing on this splitter plate be performed at Mach 0.8 or lower**.

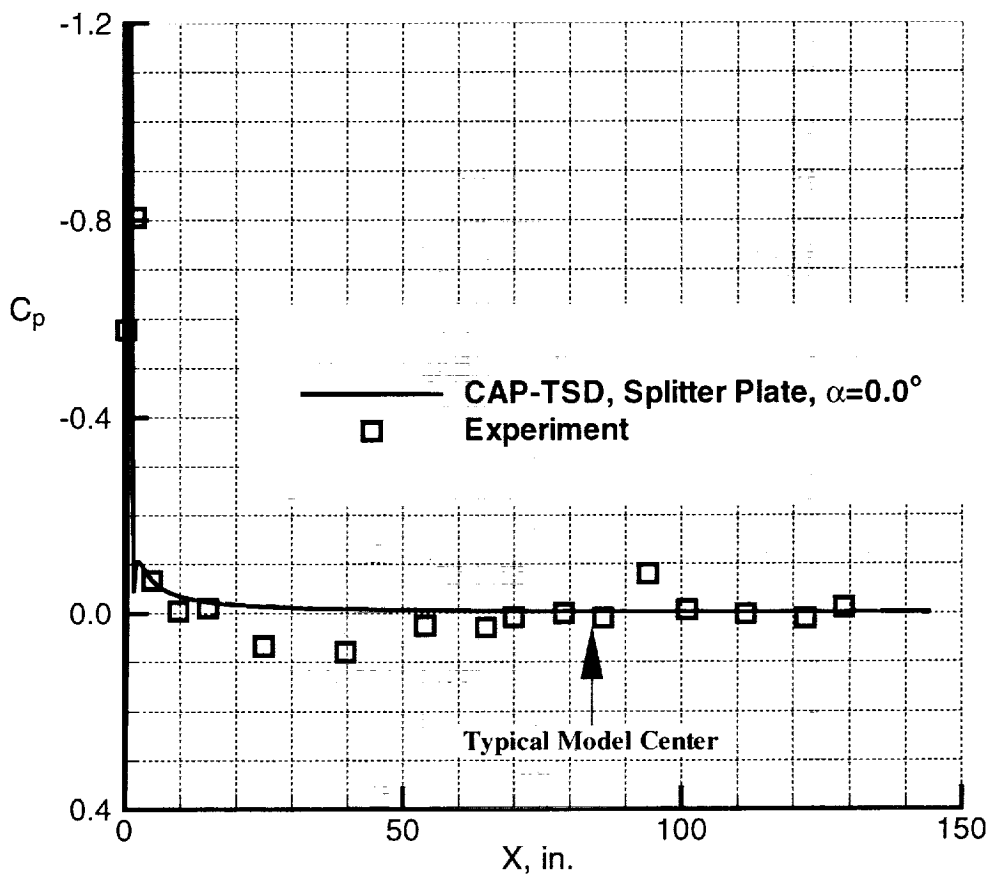

Figure 14. Comparison of CAP-TSD analysis and TDT pressure distribution at M = 0.80, q=170 psf in R-134a.

To further illustrate the impact of transonic effects on the plate pressure distribution, pressure distributions at Mach 0.9 and 0.96 are presented in Figures 15 and 16, respectively. Again only the pressure distribution along the center row of the plate is shown in these figures, and CAP-TSD results are presented for reference. At Mach 0.9, a shock is clearly present in both the CAP-TSD analysis, and the experimental data. The local experimental Mach number is as high as 1.3 at this condition and the Mach number at the last point before the shock is 1.1. This is still a relatively weak-shock case, but the flow ahead of the model is significantly displaced from freestream conditions. The shock and the general nature of the flow ahead of the model have teamed to significantly accelerate, and then decelerate the flow ahead of the model. Aerodynamic testing under these conditions would be considered high risk for acquisition of quality data. At Mach 0.96, the aerodynamic data indicate that the splitter plate is further imbedded in the transonic flow regime. The shock is considerably stronger and displaced farther aft on the plate than at 0.90. The CAP-TSD analysis places the shock well aft of the experimental location, which is typical of inviscid potential flow calculations involving strong shocks. At these conditions, the flow along the plate has experienced considerable total pressure losses, and the effectiveness of the splitter plate is severely degraded.

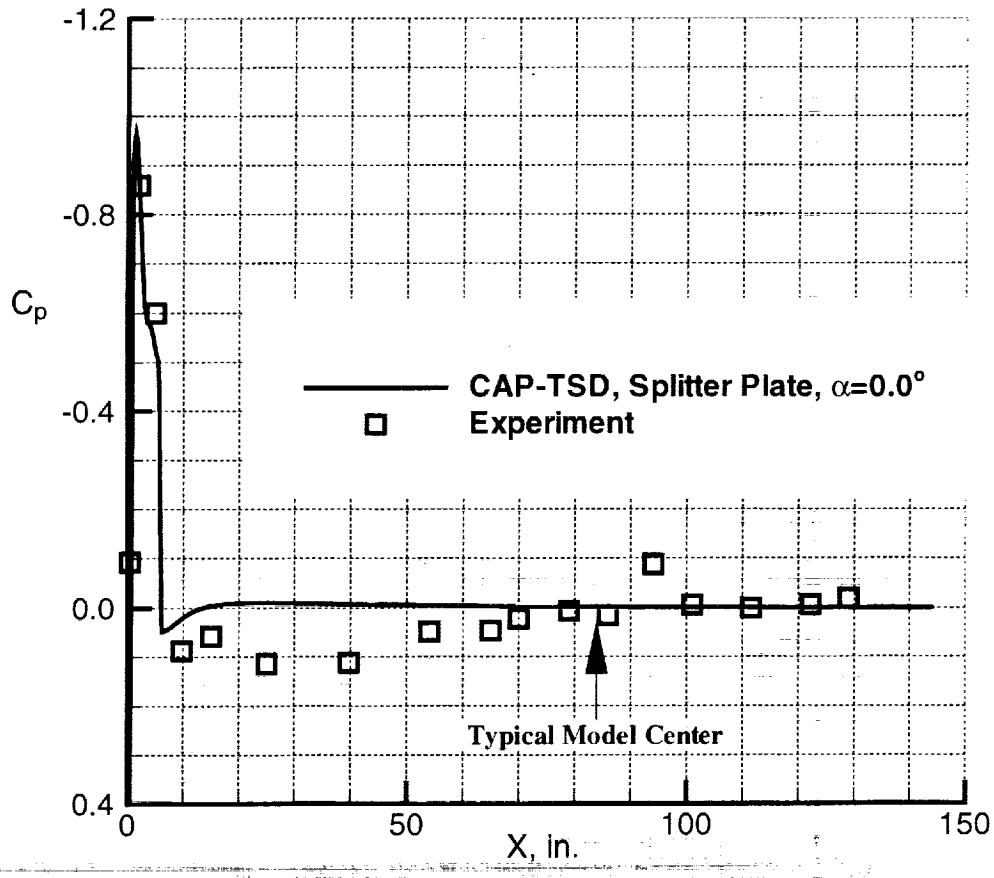

Figure 15. Comparison of CAP-TSD analysis and TDT pressure distribution at M = 0.90, q=170 psf in R-134a.

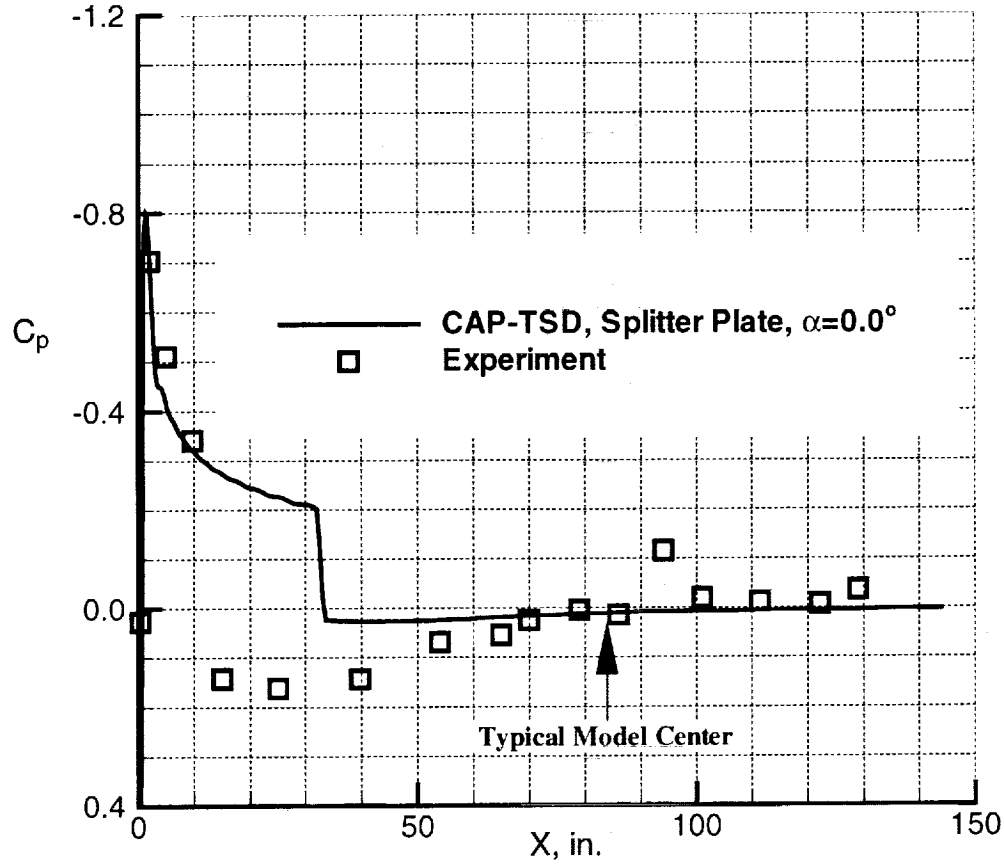

Figure 16. Comparison of CAP-TSD analysis and TDT pressure distribution at M = 0.96, q=170 psf in R-134a.

Supersonic pressure distributions were also acquired during this test, but they have little value in assessing the flow on the plate. At supersonic conditions, virtually the entire pressure distribution along the plate is displaced from the freestream pressure and with significant pressure gradients. **In short, the splitter plate is not suitable for aerodynamic tests at supersonic conditions**.

Boundary Layer Characteristics on the Splitter Plate

Boundary layer rake data acquired during this test serves two purposes. First, it quantifies the thickness of the viscous boundary layer at the model location and documents its growth as a function of flow condition. Second, it further reinforces the conclusions drawn in the previous discussion of the plate surface pressure distribution. Boundary layer data was acquired in separate runs from the previously described pressure data to eliminate interference questions on these data due to the presence of the boundary layer rake. The rake was originally intended to measure the boundary layer on the walls, floor, and ceiling of the TDT. These profiles are considerably thicker than those measured on the splitter plate, so many of the tubes in the rake simply measured freestream flow. However, there are enough tubes within the boundary layer at all flow conditions to obtain a good qualitative, if not quantitative, picture of the splitter plate boundary layer.

As with the pressure data, the boundary layer data analysis will be initiated with the Mach 0.6 R-134a data at a dynamic pressure of 170 psf. The ratio of the local velocity to freestream velocity is plotted as a function of normal distance from the plate surface in Figure 17. From this figure, it is readily observed that the overall boundary layer thickness is approximately 1.25 inches at these flow conditions. In comparison, the thickness of the TDT sidewall boundary layer is approximately 12 inches. This comparison alone demonstrates the utility of the splitter plate. The amount of any semispan model that would be immersed in boundary layer flow is considerably smaller when mounted on the splitter plate as compared to the TDT sidewall. This greatly reduces the wall interference on semispan wind tunnel models. A more meaningful quantity for aerodynamic calculations is the boundary layer displacement thickness. The displacement thickness can be physically described as the distance the inviscid streamline at the surface of the plate would be displaced by the presence of the viscous boundary layer. Many inviscid computations account for viscous effects by adding the displacement thickness to aerodynamic contours to simulate an effective viscous surface. The displacement thickness for the boundary layer profile of Figure 17 is only 0.191 inches.

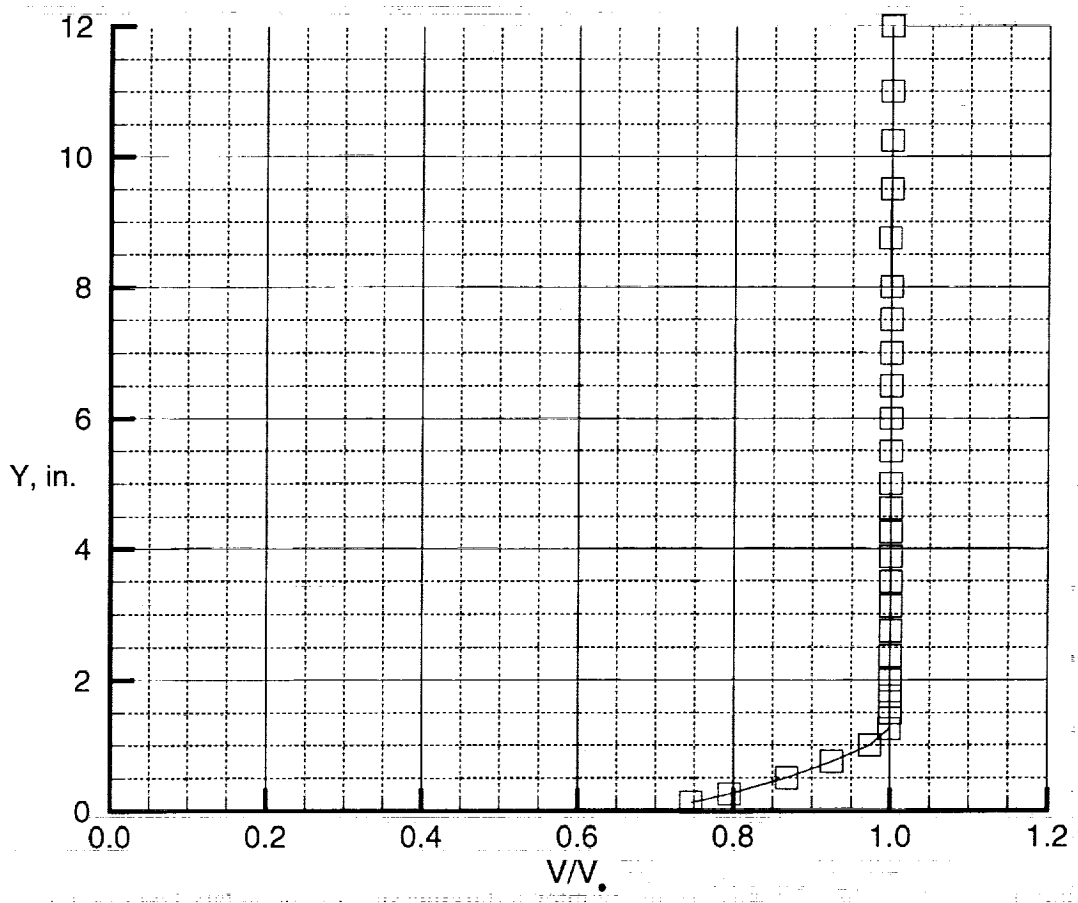

Figure 17. TDT splitter plate boundary layer profile in R-134a at Mach 0.60, q=170 psf.

The boundary layer profile at Mach 0.70 is shown in Figure 18. In this case the boundary layer thickness has increased to approximately 1.5 inches, and the computed displacement thickness is 0.198 inches. Like the previous boundary layer at Mach 0.60, this profile is very well behaved and recovers smoothly to the freestream boundary. The profile at Mach 0.80, displayed in Figure 19, shows a marked increase in the boundary layer thickness to nearly 3.0 inches. Similarly the displacement thickness for this profile increases by nearly 50 percent to 0.290 inches. At these conditions, the boundary layer is still well behaved, smoothly accelerating to the freestream velocity. However, recalling the previous discussion of the plate pressure distributions, an upper Mach number limit of 0.80 had been established for meaningful aerodynamic testing. This guideline was recommended based on the fact that flow near the leading edge of the plate had become supercritical, indicating the onset of transonic effects in this region. The sudden increase in the boundary layer thickness at Mach 0.80 appears to further reinforce this conclusion.

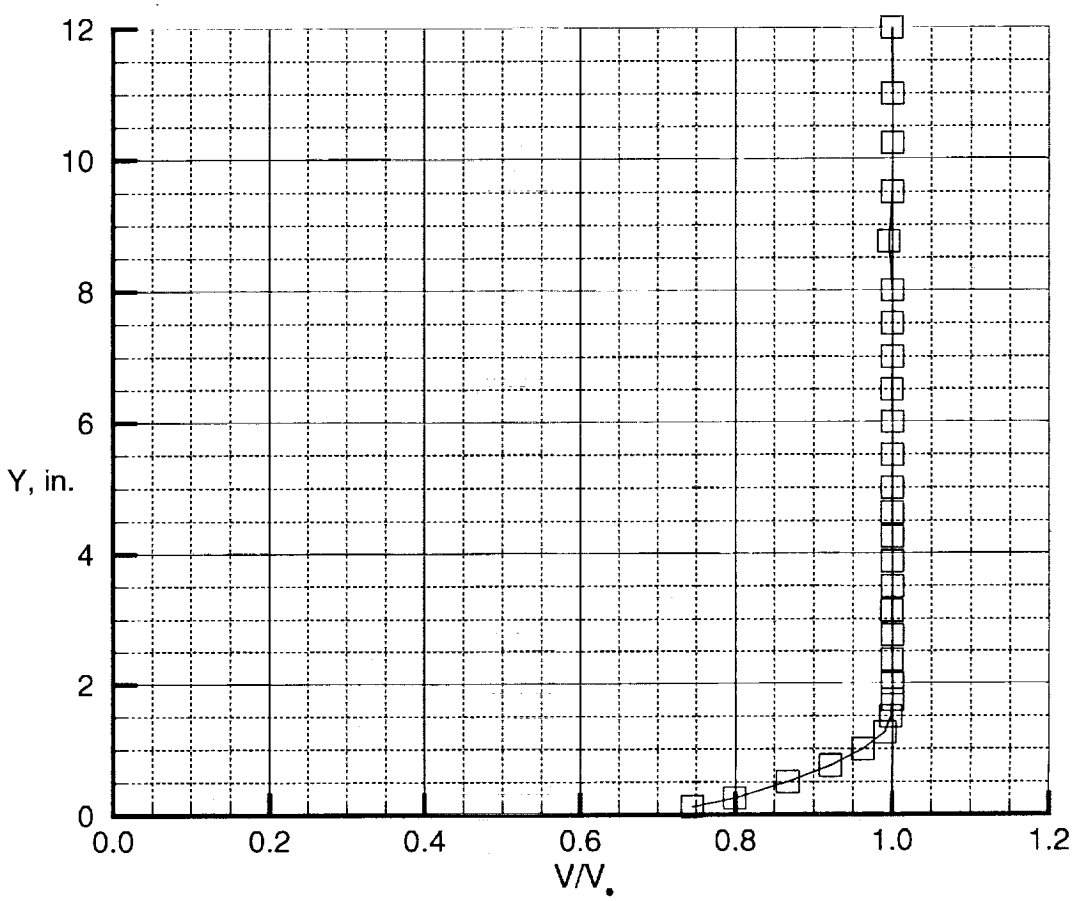

Figure 18. TDT splitter plate boundary layer profile in R-134a at Mach 0.70, q=170 psf.

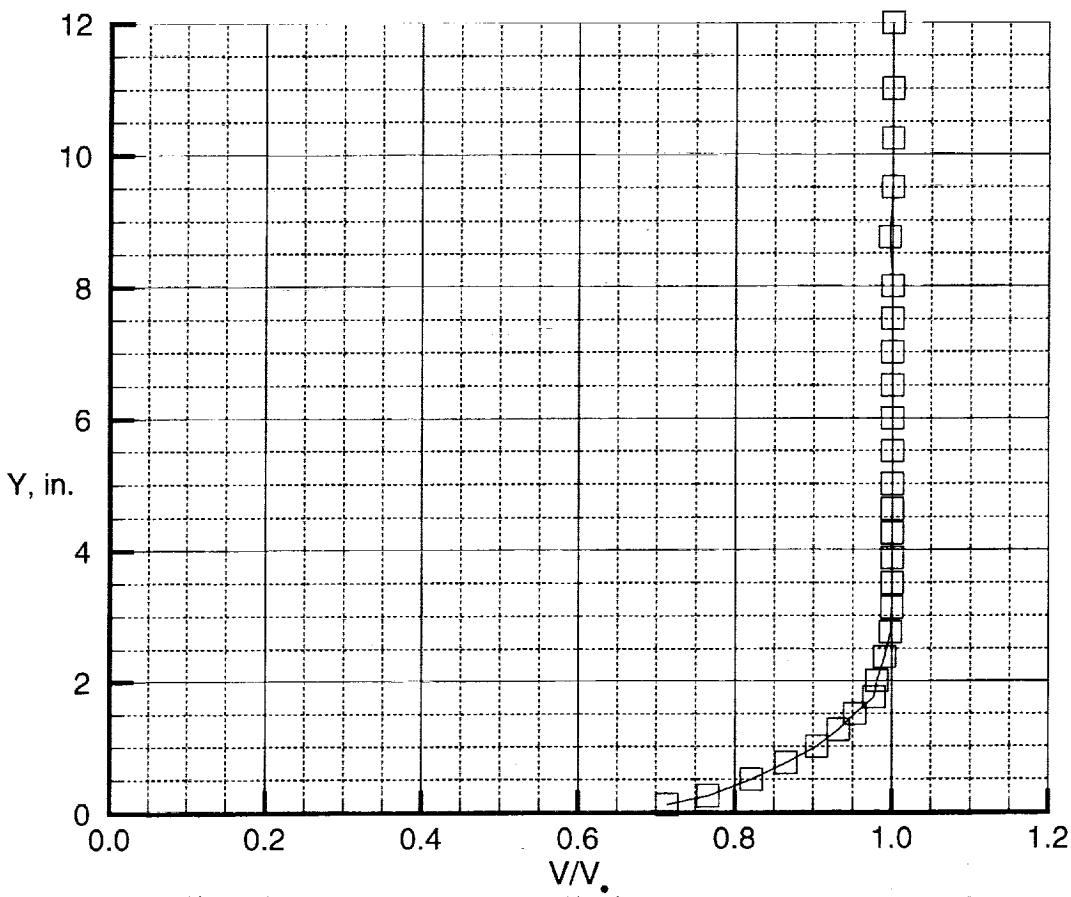

Figure 19. TDT splitter plate boundary layer profile in R-134a at Mach 0.80, q=170 psf.

Unmistakable evidence of upstream transonic effects is apparent in the boundary layer profile at Mach 0.85, shown in Figure 20. Here we see an inflection point in the boundary layer profile about 3.5 inches from the plate surface. At approximately 1.75 inches, the boundary layer profile appears to have reached a constant edge-velocity slightly lower than the freestream velocity. This is caused by a reduction of the freestream total pressure ahead of the boundary layer rake location in the region between the plate surface and about 4.25 inches above the surface. This reduction in total pressure is likely due to an upstream shock wave near the leading edge of the plate. Above 4.25 inches from the plate surface, the local total pressure matches the freestream pressure, and the velocity recovers to its full freestream value. This profile is an excellent example of the problems that can be caused at the model location by local transonic effects well forward on the splitter plate. This is an unacceptable situation for aerodynamic testing, and further establishes the recommended upper Mach number limit for the plate at Mach 0.80.

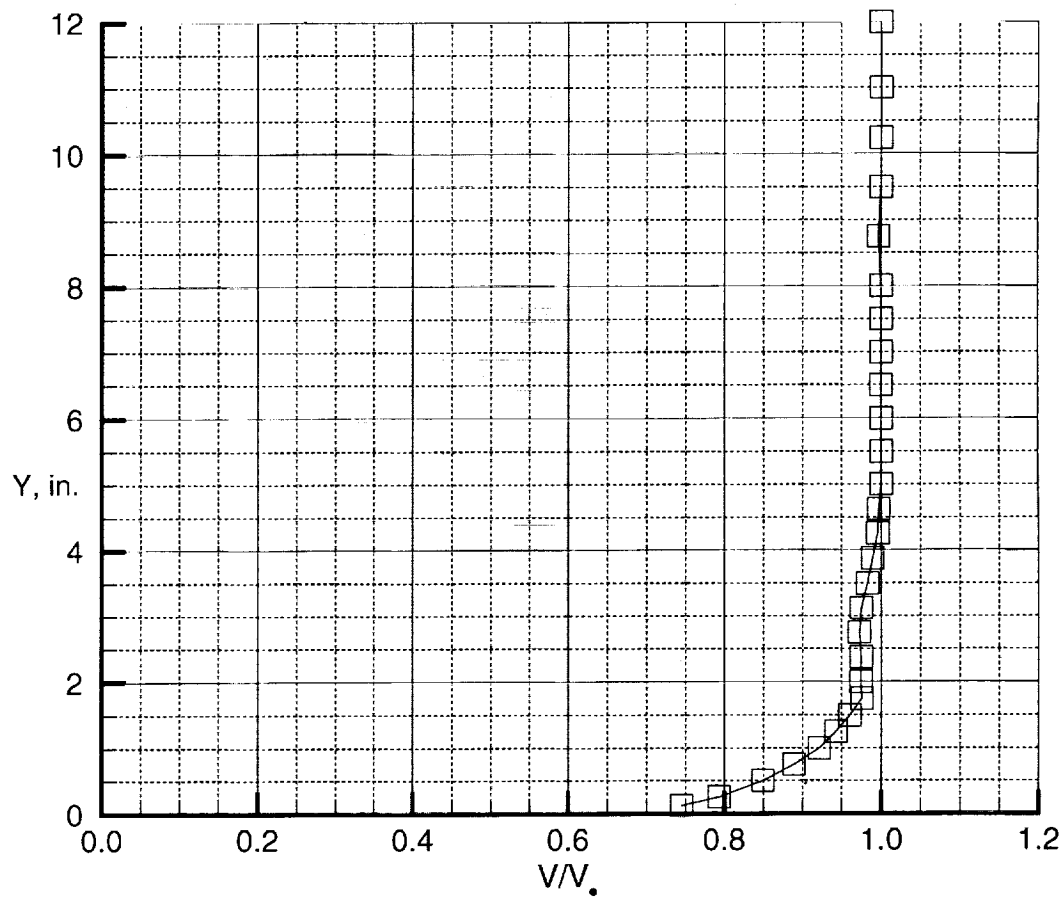

Figure 20. TDT splitter plate boundary layer profile in R-134a at Mach 0.85, q=170 psf.

A final boundary layer profile at Mach 0.90 is presented in Figure 21. In this case, upstream transonic effects influence the flow at the model location to nearly 10 inches from the plate surface. The boundary layer appears to reach a fairly constant edge velocity at about 1.75 inches from the plate surface, but this edge velocity continues to wander below the freestream velocity up to about 9.5 inches from the plate surface. Recalling that a shock wave near the leading edge of the plate was clearly evident in both the experimental data and the CAP-TSD computations at this condition, see Figure 15, this wandering of the freestream pressure can be confidently attributed to these local upstream transonic effects.

The boundary layer rake data verifies that the plate boundary layer is significantly thinner than that of the typical east wall boundary layer in the TDT. The displacement thickness is on the order of 0.2 – 0.3 inches for Mach numbers up to 0.8. Above Mach 0.8, transonic effects are discernable in the boundary layer profiles. Specifically, a reduction in the total pressure ahead of the model station results in boundary layer profiles containing inflection points and edge velocities that do not attain freestream values. This loss in total pressure is attributed to shock waves that form on the plate upstream.

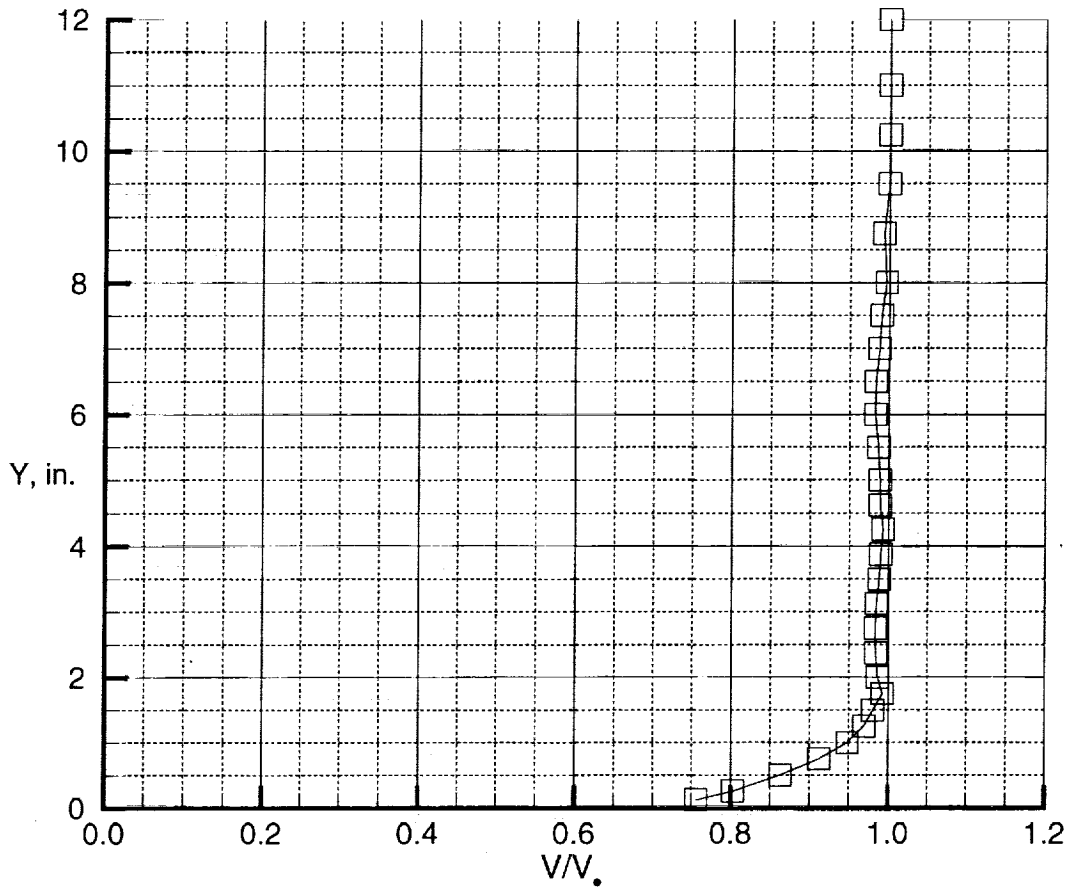

Figure 21. TDT splitter plate boundary layer profile in R-134a at Mach 0.90, q=170 psf.

Equipment Fairing Pressure Distribution

The final set of data acquired and evaluated during this test was the static pressure distribution along the centerline of the instrumentation equipment fairing previously described in Figrues 4 and 6. The purpose of these measurements was to determine the overall qualities of the flow over the fairing. Questions pertaining to the existence and formation of shocks and separated flow on the equipment fairing were the primary target of this investigation. The equipment fairing was designed to function as a conduit through which model mounting hardware and instrumentation connections could pass from the splitter plate to the TDT sidewall and be protected from the flow behind the splitter plate. The contour of this fairing is loosely based on a 37.5% thick biconvex airfoil.

This data analysis is initiated at the lowest Mach number tested during this investigation. Figure 22 shows the equipment fairing pressure distribution at Mach 0.34 and a dynamic pressure of 60 psf. This subcritical case is presented to establish a baseline characterization of the equipment fairing pressure distribution for further comparisons. There are several features of note in this figure. Even though the intended shape of the equipment fairing is a symmetrical airfoil section, the pressures indicate that the fairing generates a download as it was mounted in the TDT for this test and this loading is observed at all test conditions. This characteristic is likely due to a small nose-down angle-of-attack incurred when

mounting the fairing, and asymmetries in the overall construction of the fairing. There is also a sharp increase in the both the upper and lower surface pressures at approximately 70 percent chord. The fairing is constructed of several reinforced sheet metal sections. The center sections which connect the leading and trailing edge portions have a crease in the sheet metal on both the upper and lower surfaces which account for this sharp increase in pressure. The final characteristic to note in this and subsequent figures is the pressure recovery at the trailing edge of the fairing and the sudden decrease in pressure starting at about 92 percent chord. This sudden decrease in pressure indicates trailing edge separation of the boundary layer. At these conditions, the flow remains attached to 92 percent chord and then separates. At higher Mach numbers, this separation moves forward.

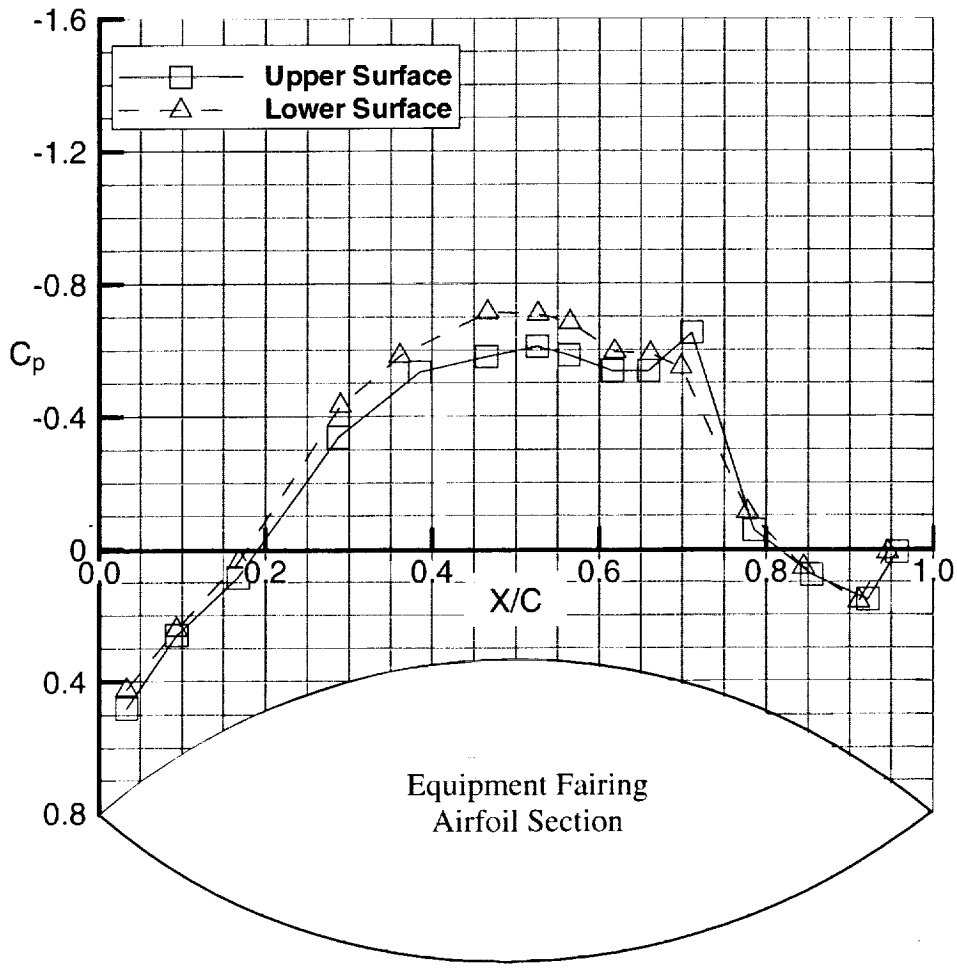

Figure 22. Equipment fairing pressure distribution, M = 0.34, q=60 psf in R-134a.

Figure 23 shows the equipment fairing pressure distribution at Mach 0.6 and a dynamic pressure of 170 psf. At these conditions, the flow remains well below Mach 1 over the entire equipment fairing surface. The overall character of the flow is the same as at Mach 0.34, with the trailing edge pressure recovery flattening significantly. This is a sign of the flow over the aft portion of the equipment fairing straightening out due to the thickening of the boundary layer. At these conditions, more severe trailing edge separation is imminent.

At Mach 0.7, shown in Figure 24, the local velocity on the upper and lower surfaces reach values very near Mach 1, thus these conditions represent those at which the equipment fairing begins to cross into the

transonic flow regime. It should be noted that, in reality, it is impossible to accurately estimate the local Mach number on the surface of the equipment fairing due to the fact that there are likely significant total pressure losses resulting from the flow around the mounting rods ahead of the fairing. The local Mach number is estimated by assuming an isentropic relationship between the static pressure and Mach number, assuming that the total pressure is the same as that of the freestream. It is recognized that this is very likely not the case for the flow behind the splitter plate. The important characteristic to note is that the flow is now separated from about 80 percent chord aft on both the upper and lower surfaces.

The final flow condition to be discussed is at Mach 0.8, shown in Figure 25. Here the flow character has changed completely from previous plots. The flow is well into the transonic regime on both the upper and lower surfaces of the fairing. The boundary layer is separated from 80 percent chord aft and the pressure distribution is not nearly as smooth as at the lower Mach numbers. There are now two distinct peaks in the pressure distribution at approximately 46 and 70 percent chord.

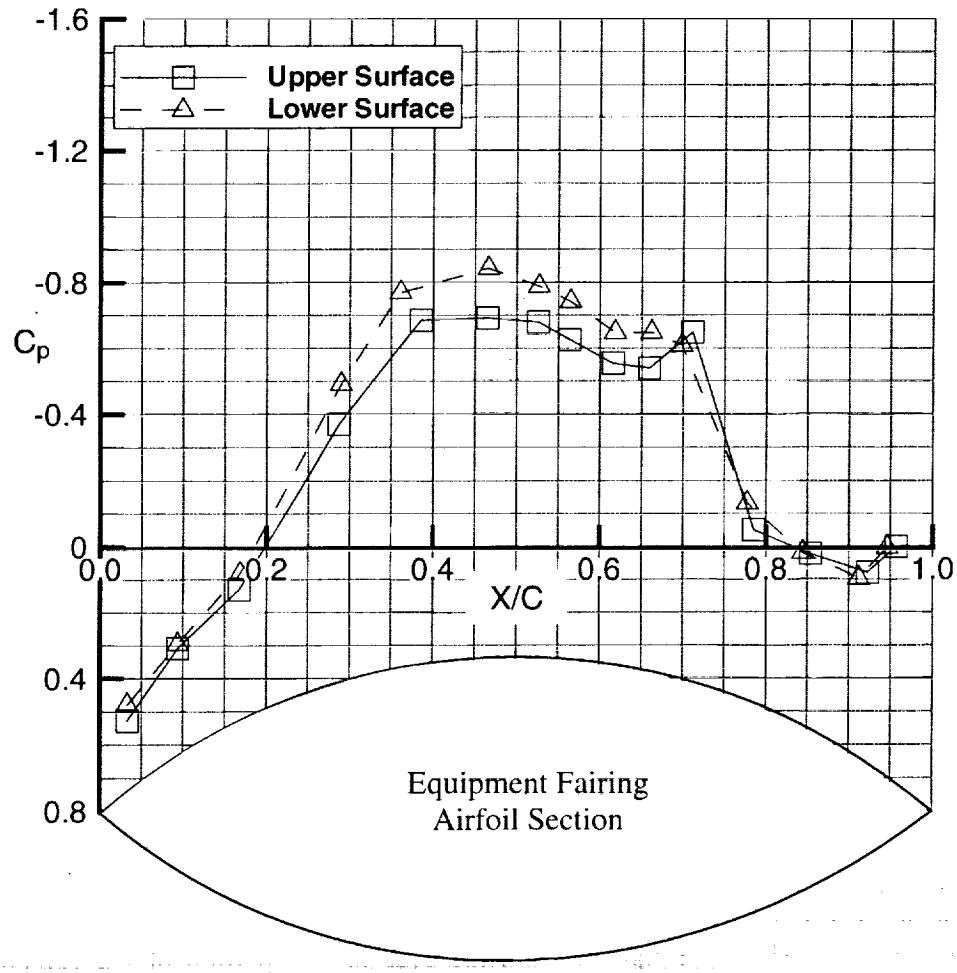

Figure 23. Equipment fairing pressure distribution, M = 0.60, q=170 psf in R-134a.

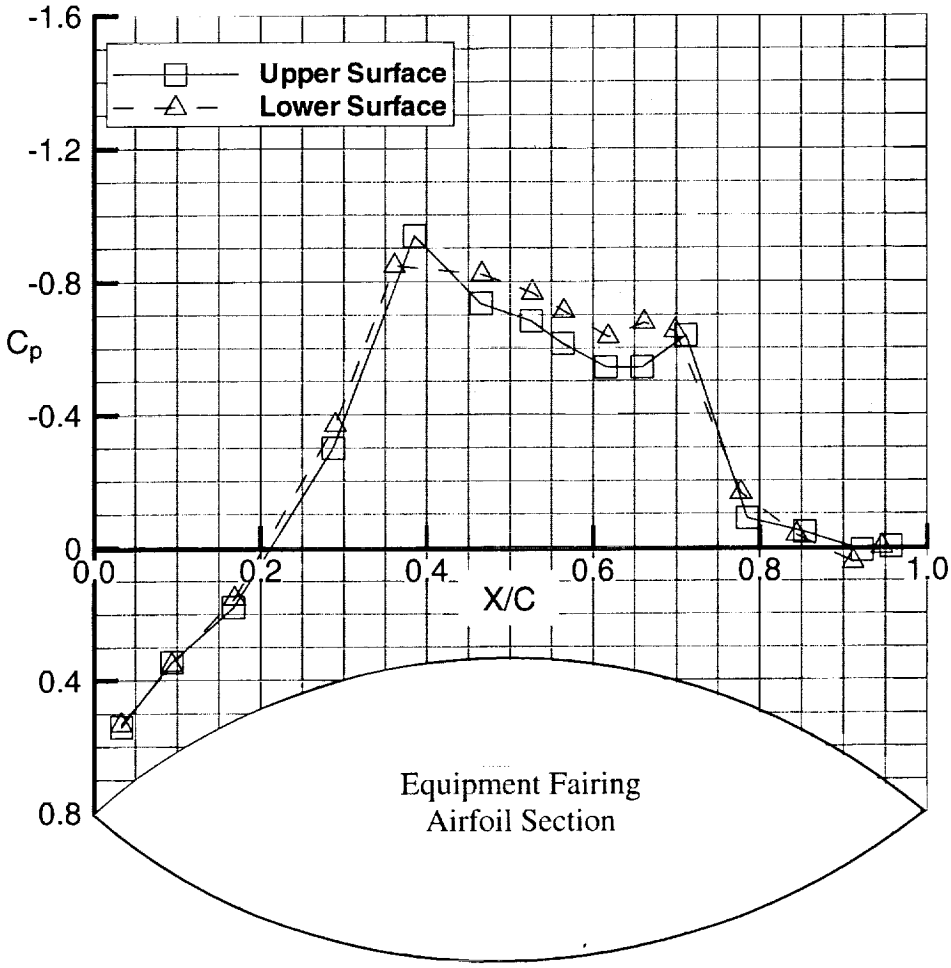

Figure 24. Equipment fairing pressure distribution, M = 0.70, q=170 psf in R-134a.

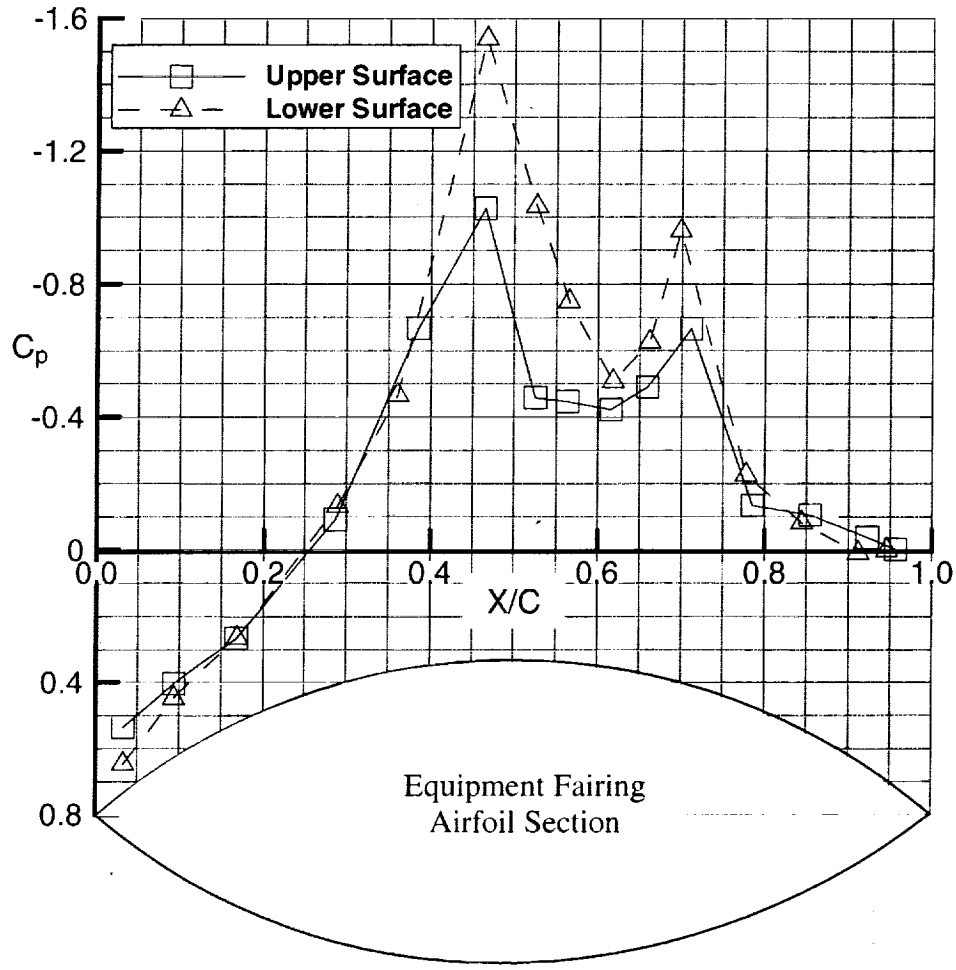

Figure 25. Equipment fairing pressure distribution, M = 0.80, q=170 psf in R-134a.

There are two important pieces of information that are inferred from this series of plots. First, the flow behind the plate exhibits transonic behavior beginning somewhere between Mach 0.7 and 0.8. Thus we can expect shock waves and potentially severe aerodynamic interference issues to begin to be observed at Mach numbers beyond this value. Second the flow is separated to some degree at all conditions, and it is severely separated at conditions beyond Mach 0.6. Even though the equipment fairing is located behind the splitter plate, both of these characteristics could have consequence to the overall flow in the test section. Transonic, separated flows are notoriously unsteady. As the flow moves deeper into the transonic regime, the shocks and separated zones probably block the path of the flow behind the plate and force more flow around the edges of the plate into the test section. If, in addition, these transonic effects are unsteady, then this unsteadiness could be experienced at the model location. Given the constraints imposed by having to securely mount the plate to the wall and shield instrumentation running between the plate and the TDT plenum chamber, it is difficult to avoid these types of problems. However, improvement to the setup behind the plate could delay the onset of these phenomena.

TESTING GUIDELINES AND RECOMMENDATIONS

The data presented in this report can be used to assist the test engineer in designing and conducting tests in the TDT using this splitter plate mount system. Most importantly, it defines flow conditions beyond which quantitative aerodynamic data becomes suspect. The recommended operating envelope for the TDT using the R-134a test medium and with the splitter plate installed is summarized in Figure 26. Both the plate pressure distribution data and the measured boundary layer data indicate that the cutoff Mach number for quantitative aerodynamic testing should be established at Mach 0.8. The data acquired at lower dynamic pressures and in air were similar in character to the R-134a test medium data at a dynamic pressure of 170 psf, so this limitation is recommended for all conditions in both air and R-134a. This does not imply that meaningful tests cannot be performed on the splitter plate beyond Mach 0.8. Good qualitative data can probably be obtained at conditions up to Mach 0.90 – 0.95. At conditions between Mach 0.80 and 0.95, the flow on the plate demonstrates a relatively flat pressure distribution at near-freestream conditions in the vicinity of the model location and the boundary layer is still relatively thin. However, it must be recognized that shock waves exist ahead of the model and the total pressure at the model location will not be the same as that in the freestream flow and may, in fact, experience relatively severe gradients. This makes accurate, quantitative interpretation of the data on the model extremely difficult. Testing at conditions above Mach 0.95 is not recommended since the flow has been severely altered by shock waves and a rapidly growing boundary layer on the forward portion of the splitter plate.

The data defining the reduction in the tunnel operating boundary due to the addition of the splitter plate and the equipment fairing pressure data actually help define potential methods for improving the performance of the current splitter plate or methods for designing a new splitter plate. The 12.5 percent reduction in the maximum attainable Mach number in the tunnel indicates that blockage due to the splitter plate and its mounting system is not negligible. Therefore, anything that can be done to reduce the physical or aerodynamic interference blockage of the plate should extend its effective range of operation. There are two obvious approaches to this problem, modify the current splitter plate, or design and fabricate a new splitter plate mounting system.

The most economical approach may be to simply modify the current plate, and there are a number of relatively simple fixes that could be implemented to improve the flow in the tunnel. However, the overall geometry and layout of the plate will ultimately determine the effectiveness of these modifications. The first, and simplest, modification would be to redesign the leading edge contour of the plate. Since the CAP-TSD computations presented in this report match the aerodynamic data very well in this region, this redesign could be confidently and efficiently performed using this methodology. Modification of the leading edge contour should delay the onset of transonic effects to a higher Mach number.

The equipment fairing pressure data indicates extensive trailing edge separation at the majority of test conditions of interest. The fairing consists of an extremely thick airfoil section. Maintaining clean attached flow on an airfoil with a thickness to chord ratio of this magnitude is impossible without some type of active flow control. The most obvious improvement here is to reduce the thickness to chord ratio of the fairing. This could be easily accomplished by maintaining the absolute thickness of the fairing at the model location, but extending the fairing fore and aft to the edges of the splitter plate. This modification would reduce the thickness of the fairing from 37.5 percent to 18.75 percent. It would also eliminate the upstream interference of the rods connecting the splitter plate to the wall since they would now be enclosed in the fairing. Again, computational analyses could be used to tailor the profile of the fairing to delay separation.

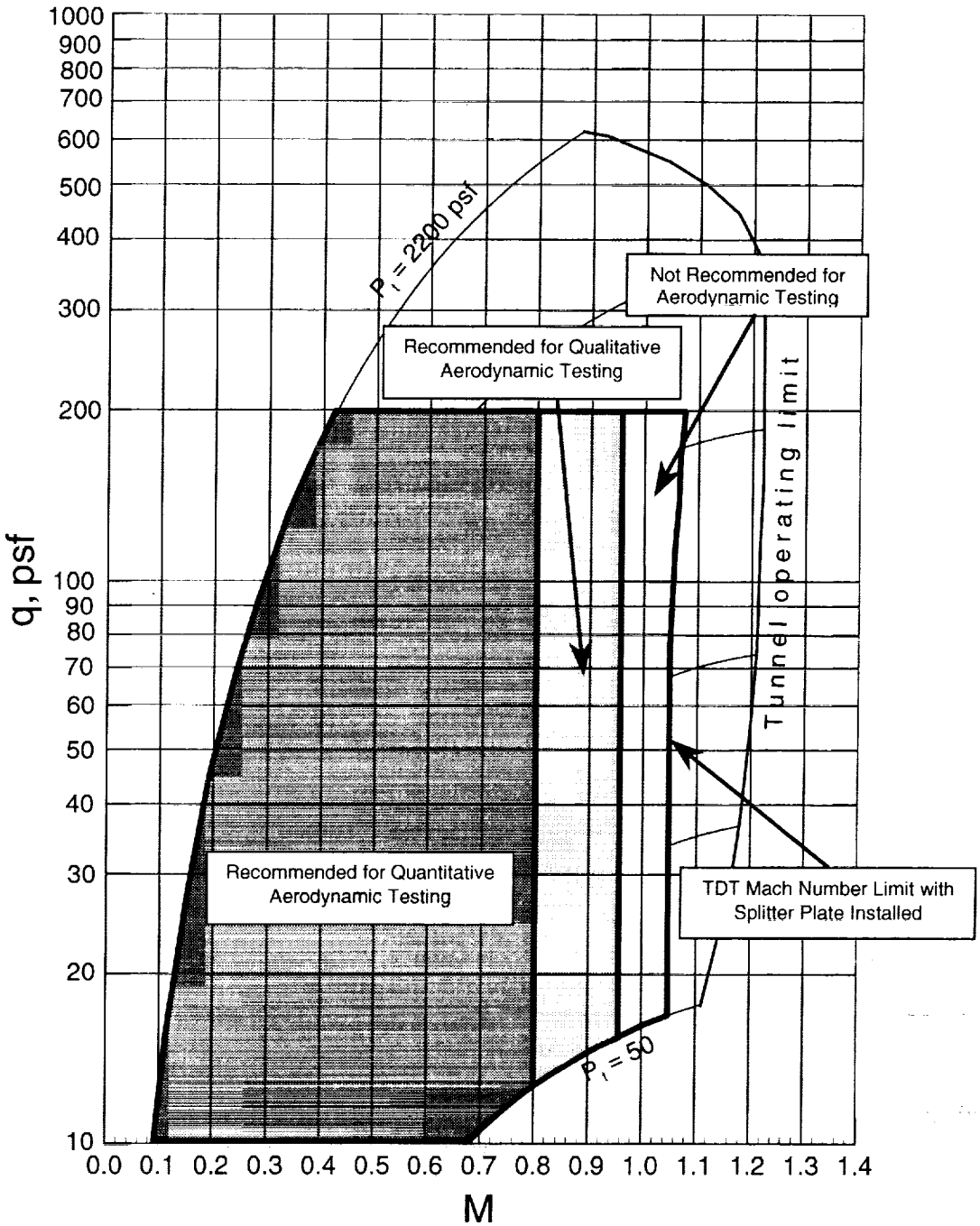

Figure 26. TDT heavy gas operational envelope with recommended area of operation using the splitter plate.

The final recommended modification would be to design and fabricate sheet metal covers that could be bolted to the upper and lower surfaces of the existing mounting rods. These plates would span the width of the rods from the TDT east wall to the back of the splitter plate and would run streamwise between the forward pair of rods and the aft pair of rods. Since the mounting rods themselves have relatively high thickness to chord ratios, flow separation on them is also a concern. These fairings would help mitigate this problem. A summary of the proposed changes to the TDT splitter plate is shown in Figure 27.

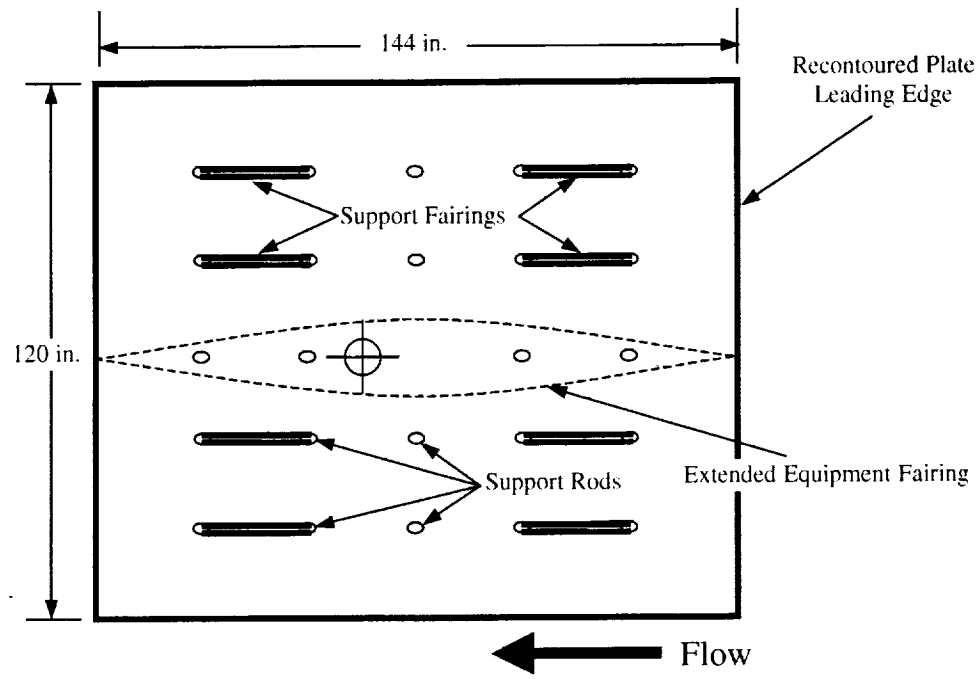

Figure 27. Proposed modifications to existing TDT splitter plate.

The TDT has undergone several changes since the original design of the splitter plate, and many of the constraints driving this design have been removed. Most notably, a retractable sidewall mounting system has been installed in the plenum chamber, allowing semispan model mounting devices of different sizes to be readily accommodated. The splitter plate as it is currently configured was designed so that a mounting device called the Pitch and Plunge Apparatus (PAPA) could be installed on a fixed turntable mount. The required dynamics of the PAPA set the distance between the turntable and the model, and thus determined the distance that the splitter plate had to be displaced from the TDT east wall. The ability to variably retract the mount behind the tunnel sidewall eliminates this problem since the distance between the model and the east wall can now be readily adjusted. Therefore, a new splitter plate, which is located significantly closer to the sidewall, could be fabricated. Previously quoted TDT east wall boundary layer measurements indicate that the splitter plate could be attached on the order of 12 inches from the east wall. Mounting the plate closer to the wall has the primary advantage of reducing the frontal area of the splitter plate and its mounting hardware. This should relieve some of the blockage effects of the splitter plate. By redesigning the support structure, the existing plate could be brought closer to the east wall, and the fabrication of a new plate could be avoided.

Finally, another possible solution to the problem is to remove the plate entirely and use pneumatic flow control to modify the flowfield along the TDT sidewall. From a productivity standpoint, this is a desirable solution since it eliminates the requirement for installation of additional hardware, namely the splitter plate, when semispan models are to be tested in the TDT. However, the substantial acquisition and maintenance costs of the flow control devices must also be factored into the tradeoffs. Pneumatic flow control comes in many different varieties. For instance, suction could be used to remove the boundary layer upstream of the model, but a conventional suction system for a wind tunnel the size of the TDT would have to be very powerful and extremely expensive. A more efficient approach is to utilize the concepts behind circulation control, which uses high velocity jets to modify the flow behavior and character. One approach might be to blow tangential to the east wall upstream of the model to energize the boundary layer and thus produce a thinner boundary layer profile at the model location. This technique has been used in some small-scale facilities to simulate a moving ground plane for land-vehicle testing[7,8]. As shown in Figure 28 this technique uses a small, high velocity jet to energize the boundary layer by entraining slower moving fluid in the boundary layer into a profile that actually involves local velocities higher than freestream. The blowing rate is adjusted, depending on tunnel flow conditions, to produce a thin, monotonically increasing velocity boundary layer profile at the model location. A similar setup can be used to remove the boundary layer through a slot in the wind tunnel wall as shown in Figure 29. In this case, circulation control is used to entrain and turn test section flow into a slot emptying into the plenum camber. This in turn starts a new boundary layer on the downstream edge of the slot. This profile will be thinner at the model location due to the relatively short distance over which the boundary layer develops.

Blowing and circulation control are powerful tools for energizing and diverting flow, requiring relatively small mass flow rates for effectiveness. An adjustable, high-pressure fluid source and geometrically simple components are all that are required for these systems, which contain no moving parts. The suction system described above is especially suitable for the TDT since a set of covers, similar to the existing slot covers, could be fabricated to hide the system from the freestream flow during full-span testing. Though implementation of this type of concept would require substantial modification to the TDT, improvements in flow quality and productivity may outweigh acquisition and maintenance costs. Problems associated with blockage due to the splitter plate are eliminated, and both the blowing and suction systems should help promote flow through the test section. The east wall boundary layer should be significantly thinner than for the untreated wall, or even the existing splitter plate. Finally, the system is highly adjustable allowing semispan test techniques tailored to the flow conditions in the test section to be easily developed and implemented. These techniques are very effective for subsonic low-velocity wind tunnels, but large-scale high-velocity facilities may pose unforeseen challenges in implementing this type of system. Further analysis of pneumatic flow control for large-scale transonic facilities is required.

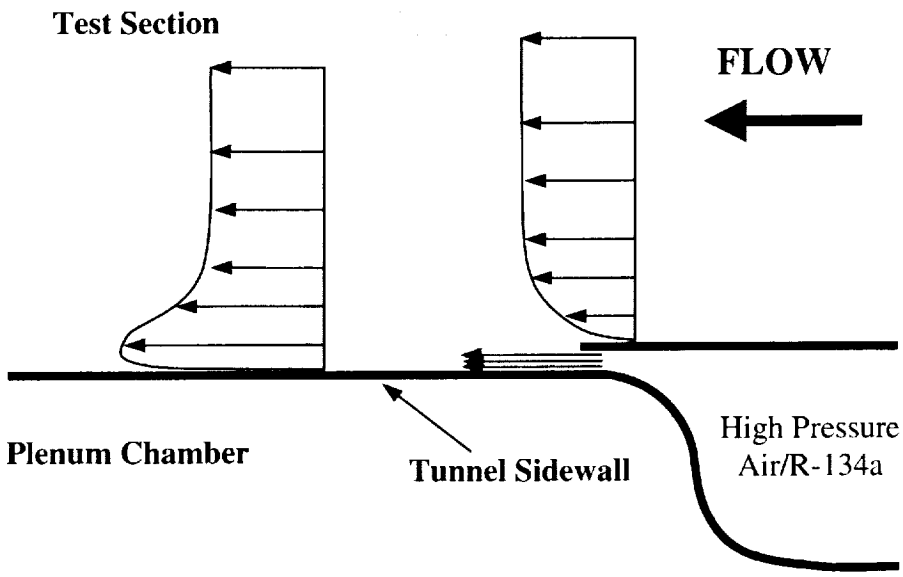

Figure 28. Tangential blowing system used to energize wind tunnel wall boundary layer.

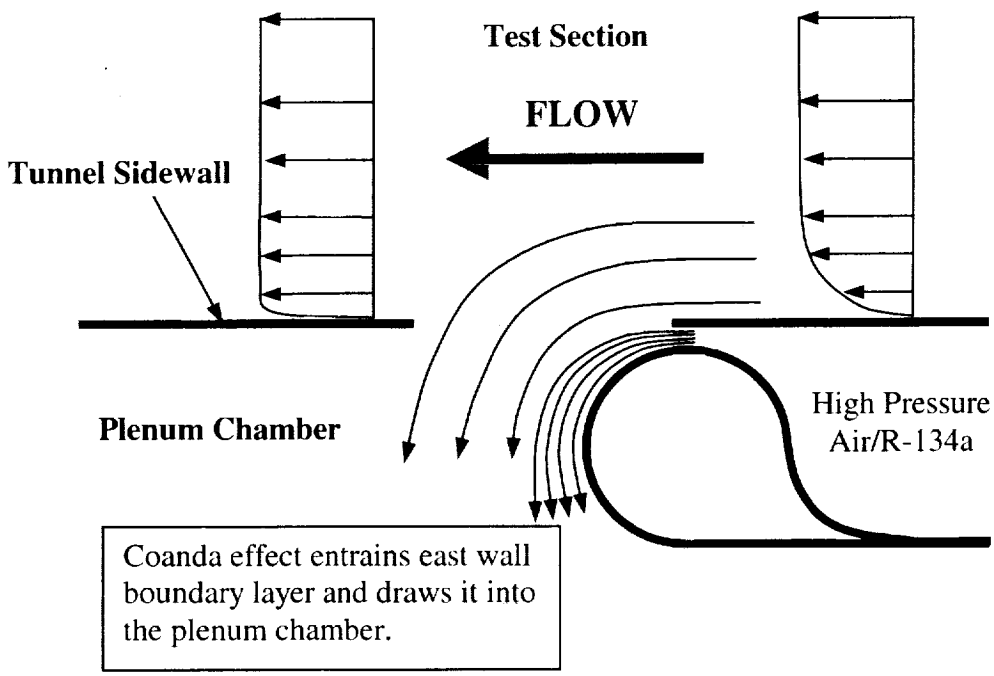

Figure 29. Circulation control suction system to remove wind tunnel wall boundary layer.

CONCLUDING REMARKS

Pressure and boundary layer rake data acquired on the NASA Langley Transonic Dynamics Tunnel splitter plate mounting apparatus have been reduced and analyzed for subsonic and transonic flows in the R-134a heavy gas test medium and air. The static pressure data acquired on the plate surface indicate that the flow in the vicinity of the model is free of pressure gradients and very close to freestream conditions until transonic effects begin to dominate the data. The flow first becomes supercritical somewhere between Mach 0.7 and 0.8, but the transonic effects at Mach 0.8 appear to be minimal making this a good upper limit for aerodynamic testing. The shape of the plate leading edge was found to be a strong player in the definition of this boundary, with locally supersonic flows near the leading edge of the plate observed at Mach numbers as low as 0.8. A shock wave near the leading edge of the plate is clearly evident at Mach 0.9. Inviscid results from the CAP-TSD transonic small disturbance code agree very well with experimental data at the leading edge of the plate and farther downstream. The CAP-TSD methodology could likely be used to assist in redesigning the leading edge of the plate in an attempt to delay its entry into the transonic flow regime. At supersonic speeds, the pressure gradients along the plate are large, and the overall pressure level is displaced from the freestream pressure making the plate unsuitable for testing in this range.

Boundary layer rake data indicate that the boundary layer on the splitter plate at the model mounting location is much thinner than on the TDT east wall. However, a sudden increase in the boundary layer thickness is observed near Mach 0.8, which seems to confirm the pressure data indication that the flow is experiencing transonic effects at these conditions. At Mach numbers of 0.85 and above the boundary layer displays evidence of upstream total pressure losses, again due to transonic effects.

The installation of the plate in the test section significantly blocks flow through the TDT. This is verified by the fact that the upper Mach number limit of the tunnel is reduced from Mach 1.2 for the empty test section to approximately Mach 1.05 with the splitter plate installed. A major contributor to this blockage is the support structure that connects the plate to the TDT east wall. The 24 support rods have relatively thick cross-section, and separated flow over each of these rods is a strong possibility. Pressures measured on the instrumentation equipment fairing exhibit at least mildly separated flow at all test conditions. The equipment fairing generates local supersonic flow at freestream conditions somewhere between Mach 0.7 and 0.8. At Mach 0.6, the separation transitions from a mild trailing edge separation to a massive separation encompassing the last 20 percent chord of the cross-section. Unsteadiness in the overall flow is of concern under these conditions.

Guidelines for testing and analyzing data acquired on this splitter plate have been formulated. These guidelines recommend that aerodynamic data acquired at Mach numbers above Mach 0.8 should only be used for qualitative analyses due to the significant potential for total pressure losses in the flowfield at the model location. The boundary layer on the plate is also considerably thicker at these conditions and above, further bringing quantitative data evaluation into question. Modifications to the existing plate have been recommended. It appears that the CAP-TSD transonic small disturbance analysis code could be useful in redesigning the leading edge contour of the plate, delaying the onset of transonic effects. Treatment of the support structure behind the plate could reduce blockage effects, and given the current retractable sidewall mounting capability in the TDT, the plate could be moved closer to the TDT east wall.

Finally, two innovative methods for removing the splitter plate from the TDT have been outlined. These methods employ pneumatic flow control concepts to treat the east wall boundary layer and reduce its thickness. A tangential blowing system, has been employed in the simulation of a moving ground plane

for ground-based vehicles, and could be adapted to simulate a symmetry plane for semispan models. This scheme energizes the existing boundary layer by injecting high velocity flow tangential to the wall surface. Using this method, the boundary layer profile at the model location can be tailored by adjusting the blowing rate. A second approach uses circulation control concepts to draw flow from the test section into the plenum chamber through a slot upstream of the model. This essentially forms a new boundary layer on the downstream edge of the slot. Since this new boundary layer has a much shorter distance to travel to the model location, it will be significantly thinner than the original east wall boundary layer. Both of these methods require significant modification to the TDT, but their potential payoffs are also significant.

In summary, the TDT splitter plate has been thoroughly tested and analyzed. The testing limitations for the plate have been established and documented. Problem areas and their sources have been identified and modifications to the existing setup have been recommended. Ideas for new semispan test techniques in the TDT have also been postulated. Should any of these recommendations be pursued further, similar testing and analysis to that described in this report should be performed to verify and document the changes made to the TDT flow character.

REFERENCES

1. Corliss, James M., and Cole, S.R., "Heavy Gas Conversion of the NASA Langley Transonic Dynamics Tunnel," AIAA Paper 98-2710, 20th AIAA Advanced Measurement and Ground Testing Technology Conference, Albuquerque, NM, June 1998.

2. Bennett, R. M., Eckstrom, C. V.; Rivera, J., A.; Dansberry, B. E.; Farmer, M. G.; and Durham, M. H.: "The Benchmark Aeroelastic Models Program - Description and Highlights of Initial Results," Paper No. 25 in Transonic Unsteady Aerodynamics and Aeroelasticity, AGARD CP 507, Mar. 1992. Also available as NASA TM-104180, 1991.

3. Rivera Jr., J. A., Dansberry, B. E.; Durham, M. H.; Bennett, R. M.; and Silva, W. A.: "Pressure Measurements on a Rectangular Wing with A NACA 0012 Airfoil During Conventional Flutter," NASA TM 104211, July 1992.

4. Dansberry, B. E., Durham, M. H.; Bennett, R. M.; Turnock, D. L.; Silva, W. A.; and Rivera Jr., J. A.: "Physical Properties of the Benchmark Models Program Supercritical Wing," NASA TM 4457, September 1993.

5. Scott, R. C., Hoadley, S. T.; Wieseman, C. D.; and Durham, M. H.: "The Benchmark Active Controls Technology Model Aerodynamic Data," AIAA Paper 97-0829, January 1997.

6. Scherer, L. B., Martin, C. A., West, M., Florance, J. P., Wieseman, C. D., Burner, A. W., and Fleming, G. A., "DARPA/AFRL/NASA Smart Wing Second Wind Tunnel Test Results," Proceedings of the SPIE 6th Annual International Symposium on Smart Structures and Materials, March 1999, included in the Proceedings

7. Wood, N. J., Roberts, L., and Ward, S., "Wind Tunnel Wall Boundary Layer Control by Coanda Jets," AIAA Paper 89-0149, January 1989.

8. Englar, R. J. and Schuster, D. M., "Experimental Evaluations of the Aerodynamics of Unlimited Racing Hydroplanes Operating In and Out of Ground Effect," SAE Paper 901869, October 1990.

REPORT DOCUMENTATION PAGE

Form Approved
OMB No. 0704-0188

Public reporting burden for this collection of information is estimated to average 1 hour per response, including the time for reviewing instructions, searching existing data sources, gathering and maintaining the data needed, and completing and reviewing the collection of information. Send comments regarding this burden estimate or any other aspect of this collection of information, including suggestions for reducing this burden, to Washington Headquarters Services, Directorate for Information Operations and Reports, 1215 Jefferson Davis Highway, Suite 1204, Arlington, VA 22202-4302, and to the Office of Management and Budget, Paperwork Reduction Project (0704-0188), Washington, DC 20503.

1. AGENCY USE ONLY (Leave blank)

2. REPORT DATE
March 2001

3. REPORT TYPE AND DATES COVERED
Technical Memorandum

4. TITLE AND SUBTITLE
Aerodynamic Measurements on a Large Splitter Plate for the NASA Langley Transonic Dynamics Tunnel

5. FUNDING NUMBERS
WU 706-31-41-02

6. AUTHOR(S)
David M. Schuster

7. PERFORMING ORGANIZATION NAME(S) AND ADDRESS(ES)
NASA Langley Research Center
Hampton, VA 23681-2199

8. PERFORMING ORGANIZATION REPORT NUMBER
L-18054

9. SPONSORING/MONITORING AGENCY NAME(S) AND ADDRESS(ES)
National Aeronautics and Space Administration
Washington, DC 20546-0001

10. SPONSORING/MONITORING AGENCY REPORT NUMBER
NASA/TM-2001-210828

11. SUPPLEMENTARY NOTES

12a. DISTRIBUTION/AVAILABILITY STATEMENT
Unclassified-Unlimited
Subject Category 05 Distribution: Standard
Availability: NASA CASI (301) 621-0390

12b. DISTRIBUTION CODE

13. ABSTRACT (Maximum 200 words)
Tests conducted in the NASA Langley Research Center Transonic Dynamics Tunnel (TDT) assess the aerodynamic characteristics of a splitter plate used to test some semispan models in this facility. Aerodynamic data are analyzed to determine the effect of the splitter plate on the operating characteristics of the TDT, as well as to define the range of conditions over which the plate can be reasonably used to obtain aerodynamic data. Static pressures measurements on the splitter plate surface and the equipment fairing between the wind tunnel wall and the splitter plate are evaluated to determine the flow quality around the apparatus over a range of operating conditions. Boundary layer rake data acquired near the plate surface define the viscous characteristics of the flow over the plate. Data were acquired over a range of subsonic, transonic and supersonic conditions at dynamic pressures typical for models tested on this apparatus. Data from this investigation should be used as a guide for the design of TDT models and tests using the splitter plate, as well as to guide future splitter plate design for this facility.

14. SUBJECT TERMS
Aerodynamics; Splitter plate; TDT; Flow quality; Dynamic pressure

15. NUMBER OF PAGES
42

16. PRICE CODE
A03

17. SECURITY CLASSIFICATION OF REPORT	18. SECURITY CLASSIFICATION OF THIS PAGE	19. SECURITY CLASSIFICATION OF ABSTRACT	20. LIMITATION OF ABSTRACT
Unclassified	Unclassified	Unclassified	UL